

**A ONE-DIMENSIONAL VISCOELASTIC MODEL FOR ICE**

**BY**

**J. F. DORRIS**

**TECHNICAL INFORMATION RECORD**

**BRC-1451  
JULY 1986**

**Project No. 370-27802.00  
Arctic Engineering**



**SHARED - Under the Research Agreement between SIRM,  
and Shell Oil Company dated January 1, 1960,  
as amended.**

**SHELL DEVELOPMENT COMPANY**

**A DIVISION OF SHELL OIL COMPANY**

**BELLAIRE RESEARCH CENTER**

**HOUSTON, TEXAS**



TABLE OF CONTENTS

	Page
Abstract.....	iv
Introduction.....	1
The One-dimensional Stress Reduction of the Nonlinear Viscoelastic Model for Ice.....	2
Laboratory Test Data.....	7
Constant Load Tests.....	8
Constant Strain Rate Tests.....	9
Construction of Data Functions.....	19
Constant Load Data Function.....	19
Constant Strain Rate Data Functions.....	23
Response Functions.....	38
Reduced Uniaxial Models.....	39
Stress-Strain Domain for Data Functions.....	46
Summary and Recommendations.....	50
References.....	51

LIST OF ILLUSTRATIONS

Figure Number		Page
1	Idealized responses for uniaxial stress tests.....	5
2	Typical fit of the assumed creep curve to experimental data.....	11
3	Family of creep curves used to construct the data functions.....	13
4	Typical fit of the assumed stress-strain curve to experimental data.....	16
5	Family of stress-strain curves used to construct the data function.....	20

Figure Number		Page
6	Calculation of the data function F from the constant load curves.....	21
7	Stress-strain domain for constant load tests.....	22
8	Mapping of the points $F(S_k, e_j)$ , $k = 1,4$ into the $e_j = \text{constant}$ plane.....	24
9	Three-dimensional representation of the F data function.....	25
10	Planes of constant strain for the F data function.....	26
11	Planes of constant stress for the F data function.....	27
12	Calculation of the Y and W data functions from the constant strain rate curves.....	28
13	Stress-strain domain for W and Y data functions.....	30
14	Mapping of the points $W(S_k, e_j)$ and $Y(S_k, e_j)$ $k = 1,4$ into the $e_j = \text{constant}$ plane.....	31
15	Three-dimensional representation of the W data function.....	32
16	Planes of constant strain for the W data function.....	33
17	Planes of constant stress for the W data function.....	34
18	Three-dimensional representation of the Y data function.....	35
19	Planes of constant strain for the Y data function.....	36
20	Planes of constant stress for the Y data function.....	37
21a	Expected creep response of ice upon unloading.....	40
21b	Expected shape of $f(e)$ .....	40
22	Three-dimensional representation of the response function $\hat{\phi}(s, e)$ based on the reduced model, $\hat{\omega}/\hat{\phi} = f(e)$ .....	43
23	Three-dimensional representation of the response function $\hat{\omega}(s, e)$ based on the reduced model, $\hat{\omega}/\hat{\phi} = f(e)$ .....	44
24	Three-dimensional representation of the response function $\psi(s, e)$ based on the reduced model, $\hat{\omega}/\hat{\phi} = f(e)$ .....	45
25	Stress-strain domains for the response functions.....	47

LIST OF TABLES

Table Number		Page
1	Constant Load Tests from Mellor and Cole Used to Generate Data Functions.....	10
2	Constants for the Approximating Functions for the Constant Load Tests.....	12
3	Constant Strain Rate Tests From Mellor and Cole Used to Generate Data Functions.....	15
4	Constants for the Approximating Functions of the Force Time Curves.....	17
5	Constants for the Approximating Functions of the Stress-Strain Curves.....	18

ABSTRACT

The one-dimensional stress reduction of a viscoelastic model of the differential type is presented. Multiaxial data are required to construct the three response functions necessary to describe the one-dimensional model. In the absence of multiaxial data, certain simplifying assumptions are made which would permit the use of uniaxial data alone. However, these assumptions lead to physically unacceptable response functions.

This report should be of interest to those who are interested in the constitutive modeling of ice.

TECHNICAL INFORMATION RECORD BRC-1451

A ONE-DIMENSIONAL VISCOELASTIC MODEL FOR ICE

BY

J. F. DORRIS

INTRODUCTION

The Mechanical Properties of Sea Ice Program is a project consisting of several phases to determine the mechanical properties of multiyear sea ice. The project was developed and administered by Shell Development Company. Participants sponsoring Phase I of the project included Amoco Production Company, Arco Oil and Gas Company, Chevron Oil Field Research Company, Exxon Production Research Company, Gulf Research and Development Company, Minerals Management Service of the Department of the Interior, Mitsui Engineering and Shipbuilding Company, Sohio Petroleum Company, and Texaco U.S.A. The experimental program in Phase I focused on defining the variation of the uniaxial compressive strength of multiyear ridge ice over the temperature, strain rate regime of most interest to the engineer. The experimental results are reported by Cox et al.<sup>1</sup>

Phase I also included a theoretical investigation into the development of a constitutive model appropriate for ice. This theoretical investigation was conducted by Professor L. W. Morland of the University of East Anglia acting as a consultant to the project. Morland<sup>2</sup> studied the one-dimensional stress reduction of the model previously developed by Spring and Morland.<sup>3</sup> The work presented here represents the application of actual test data in the construction of the one-dimensional stress model.

Current techniques used to calculate ice loads on structures employ constitutive models such as linear elasticity or perfect plasticity which fail to account for the rate dependent nature of the mechanical response of ice. Elasticity assumes a one-to-one correspondence between stress and strain independent of time while plastic limit analysis requires an a priori assumption about the strain rate to determine the appropriate yield function. In general, ice structure interaction problems should have as their solution time

dependent stresses and strains and allow for spatial variation of the strain rate. Experimental observations, such as the nonlinear creep response of ice, preclude the use of time dependent rheological models commonly employed in the theory of linear viscoelasticity. Several empirical one-dimensional constitutive laws have been proposed, but their generalization to more realistic three-dimensional situations is limited.

To describe the mechanical response of ice, Spring and Morland<sup>3</sup> develop a nonlinear viscoelastic solid model of the differential type. This model is constructed from frame indifferent tensors which satisfy the fundamental invariance principles of physics. In the development of the model, attention is focused on deriving the simplest tensor relation between the physical variables which is necessary to describe the observed response of ice under constant load (creep) and constant strain rate test conditions. As a result, a relation between stress, strain, and their rates is developed.

As part of Phase I, Morland<sup>2</sup> investigates the one-dimensional stress reduction of the tensor relation. This reduction is described by three material response functions. The response functions are related to three data functions which are constructed from a family of uniaxial constant strain rate and uniaxial constant load curves. However, these three data functions only provide two independent relations for the response functions. In fact, Morland shows that any one-dimensional test program will yield, at the most, only two independent relations for the response functions. Consequently, two-dimensional data are necessary to completely describe the one-dimensional tensor reduction.

Morland attempts to develop a one-dimensional stress model from one-dimensional data alone. Certain assumptions are made about the functional form of the response functions which permit the construction of three so-called "reduced" one-dimensional models. However, as will be seen later, these reduced models are unacceptable, and further attempts to develop a one-dimensional model are abandoned.

#### THE ONE-DIMENSIONAL STRESS REDUCTION OF THE NONLINEAR VISCOELASTIC MODEL FOR ICE

The nonlinear viscoelastic model of the differential type proposed by Spring and Morland is given without proof by the equation,

$$\underline{\underline{S}} + \psi \left[ \underline{\underline{S}}^{(1)} - \frac{2}{3} \text{tr} (\underline{\underline{S}} \underline{\underline{D}}) \underline{\underline{1}} \right] = \phi_1 \underline{\underline{D}} + \phi_2 \left[ \underline{\underline{D}}^2 - \frac{2}{3} I_2 \underline{\underline{1}} \right] \quad (1)$$

$$+ \omega_1 \left[ \underline{\underline{B}} - \frac{1}{3} K_1 \underline{\underline{1}} \right] + \omega_2 \left[ \underline{\underline{B}} - \frac{1}{3} (K_1^2 - 2K_2) \underline{\underline{1}} \right].$$

Here  $\underline{\underline{S}}$  denotes the deviatoric components of the Cauchy stress  $\underline{\underline{\sigma}}$ ,  $\underline{\underline{S}}^{(1)}$  is a frame indifferent stress rate,  $\underline{\underline{D}}$  is the rate of deformation tensor,  $\underline{\underline{B}}$  is the Cauchy-Green strain tensor, and  $\underline{\underline{1}}$  is the unit tensor. The quantities  $I_i$ ,  $J_i$ , and  $K_i$ ,  $i = 1, 3$  denote the invariants of  $\underline{\underline{D}}$ ,  $\underline{\underline{S}}$ , and  $\underline{\underline{B}}$ , respectively. The material response is described by the functions  $\psi$ ,  $\phi_1$ ,  $\phi_2$ ,  $\omega_1$ , and  $\omega_2$  which must be determined from experimental data and are, in general, functions of the variants  $J_2$ ,  $J_3$ ,  $K_1$ ,  $K_2$  and their rates.

The relation given by equation (1) is a frame indifferent differential operator law which relates stress, strain, stress rate and strain rate. It represents the lowest order differential relation necessary to describe the qualitative features of the uniaxial response of ice under constant load and constant strain rate test conditions. To simplify its derivation, the relation assumes incompressibility and initial isotropy in the reference configuration. The reader should refer to Spring and Morland<sup>3</sup> for the derivation and further discussion of equation (1).

For the uniaxial state of stress,  $\sigma_{11} = \sigma < 0$  and all other  $\sigma_{ij} = 0$ , the tensor relation in (1) becomes,

$$(1 - \epsilon)^3 \bar{\sigma} + \hat{\psi} (1 - \epsilon)^2 \left[ (1 - \epsilon) \dot{\bar{\sigma}} - 2\dot{\epsilon} \bar{\sigma} \right] = \frac{3}{2} \hat{\phi} (1 - \epsilon) \dot{\epsilon} + \hat{\omega} \epsilon, \quad (2)$$

where the superposed dot refers to the material derivative. The quantity  $\bar{\sigma}$  is the nominal stress referred to the reference configuration and is related to the Cauchy stress by  $\sigma = \bar{\sigma} (1 - \epsilon)$ . The quantity  $\epsilon$  is the longitudinal engineering strain given by  $\epsilon = (\ell_0 - \ell) / \ell_0$  where  $\ell_0$  and  $\ell$  are the reference and current longitudinal lengths, respectively. In the derivation of (2), Spring and Morland restrict the dependence of the response functions on the stress and strain invariants  $J_2$ ,  $J_3$ ,  $K_1$ ,  $K_2$  and not their rates. For uniaxial stress they become functions of  $\bar{\sigma}$  and  $\epsilon$  only. The restricted dependence is emphasized by introducing the notation,

$$\psi = \hat{\psi}(\bar{\sigma}, \epsilon), \quad \phi = \hat{\phi}(\bar{\sigma}, \epsilon), \quad \omega = \hat{\omega}(\bar{\sigma}, \epsilon)$$

The quantity  $\hat{\omega}$  is a combination of  $\hat{\omega}_1$  and  $\hat{\omega}_2$  and is given by

$$\hat{\omega}\epsilon = \hat{\omega}_1(1 - \epsilon)[1 - (1 - \epsilon)^3] + \hat{\omega}_2[1 - (1 - \epsilon)^6] = (3\hat{\omega}_1 + 6\hat{\omega}_2)\epsilon + 0(\epsilon^2) \quad (3)$$

Hence, the uniaxial stress reduction of (1) cannot distinguish between the individual contributions of  $\hat{\omega}_1$  and  $\hat{\omega}_2$ .

Equation (2) is derived with the purpose of describing the qualitative features of the idealized uniaxial constant load and constant strain rate responses illustrated in Figure 1. In Figure 1(a), the constant load response initially consists of an instantaneous elastic jump,  $\epsilon_e$ , which depends on the magnitude of the applied load. The elastic jump is followed by periods of primary, secondary, and tertiary creep which correspond to periods of decelerating, constant (or minimum), and accelerating strain rates. The secondary creep may only be an inflection point defined by the time,  $t_m$ , to minimum strain rate. In Figure 1(b), the constant strain rate response is characterized by the stress rising from zero to a peak value,  $\sigma_M$ , and then falling to an almost constant post peak value.

Following Spring and Morland,<sup>3</sup> the uniaxial response functions in (2) are constructed by considering the idealized responses from a family of constant load and constant strain rate tests. Consider first a family of constant load responses. In this case  $\dot{\bar{\sigma}} = 0$  which reduces equation (2) to an explicit expression for  $\dot{\epsilon}$  in terms of  $\bar{\sigma}$  and  $\epsilon$ , i.e.

$$\dot{\epsilon} \left[ \frac{3}{2} \hat{\phi} (1 - \epsilon) + 2\hat{\psi}\bar{\sigma}(1 - \epsilon)^2 \right] = (1 - \epsilon)^3 \bar{\sigma} - \hat{\omega}\epsilon \quad (4)$$

Since the strain response  $\epsilon(t)$  in Figure 1(a) is a monotonic function of time for a given  $\bar{\sigma}$ , the strain rate response can be expressed as a function of  $\epsilon$  rather than  $t$ . Hence the family of response curves for a range of constant  $\bar{\sigma}$  values determines a relation  $\dot{\epsilon} = F(\bar{\sigma}, \epsilon)$  for  $\epsilon \geq \epsilon_e(\bar{\sigma})$ ,  $\bar{\sigma} > 0$ . Solving for  $\dot{\epsilon}$  in (4), the data function  $F(\bar{\sigma}, \epsilon)$  is given by

$$\dot{\bar{\sigma}} = 0: \quad \dot{\epsilon} = F(\bar{\sigma}, \epsilon) = \frac{(1 - \epsilon)^3 \bar{\sigma} - \hat{\omega}\epsilon}{\frac{3}{2} \hat{\phi}_1 (1 - \epsilon) + 2\hat{\psi}\bar{\sigma}(1 - \epsilon)^2} \quad (5)$$

The data function  $F(\bar{\sigma}, \epsilon)$  is the strain rate response of the family of constant load curves and is determined by measuring the slope at various points along each curve.

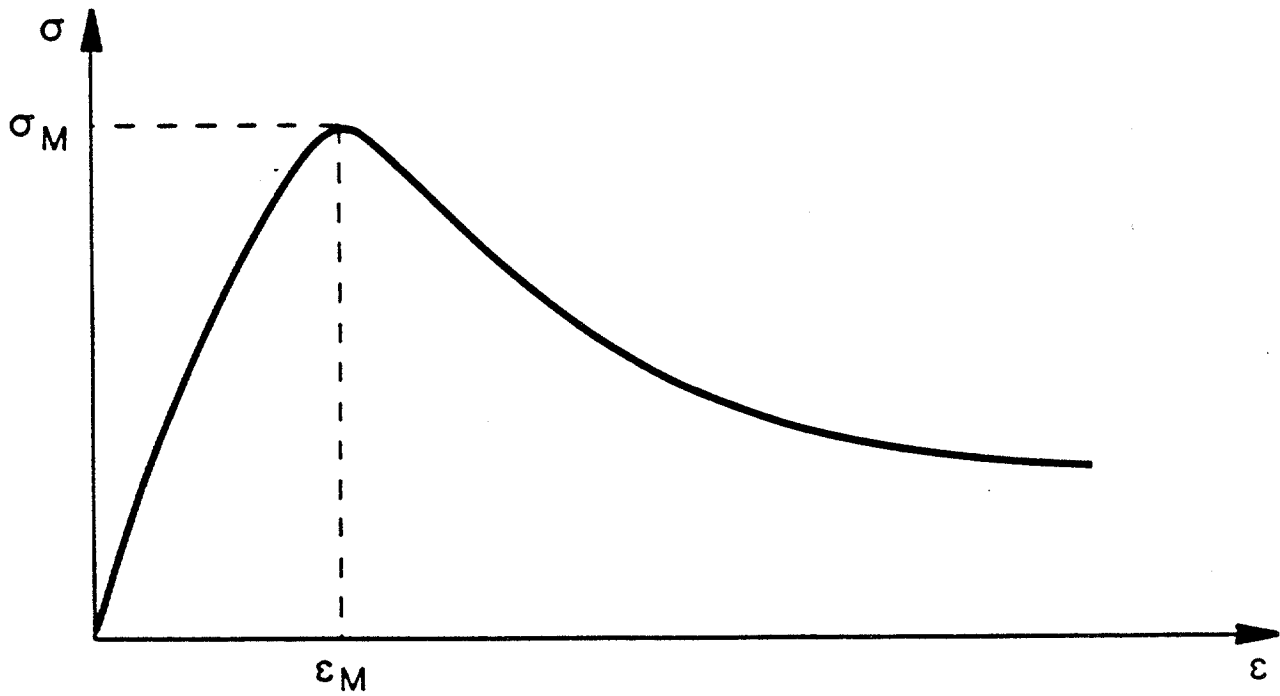
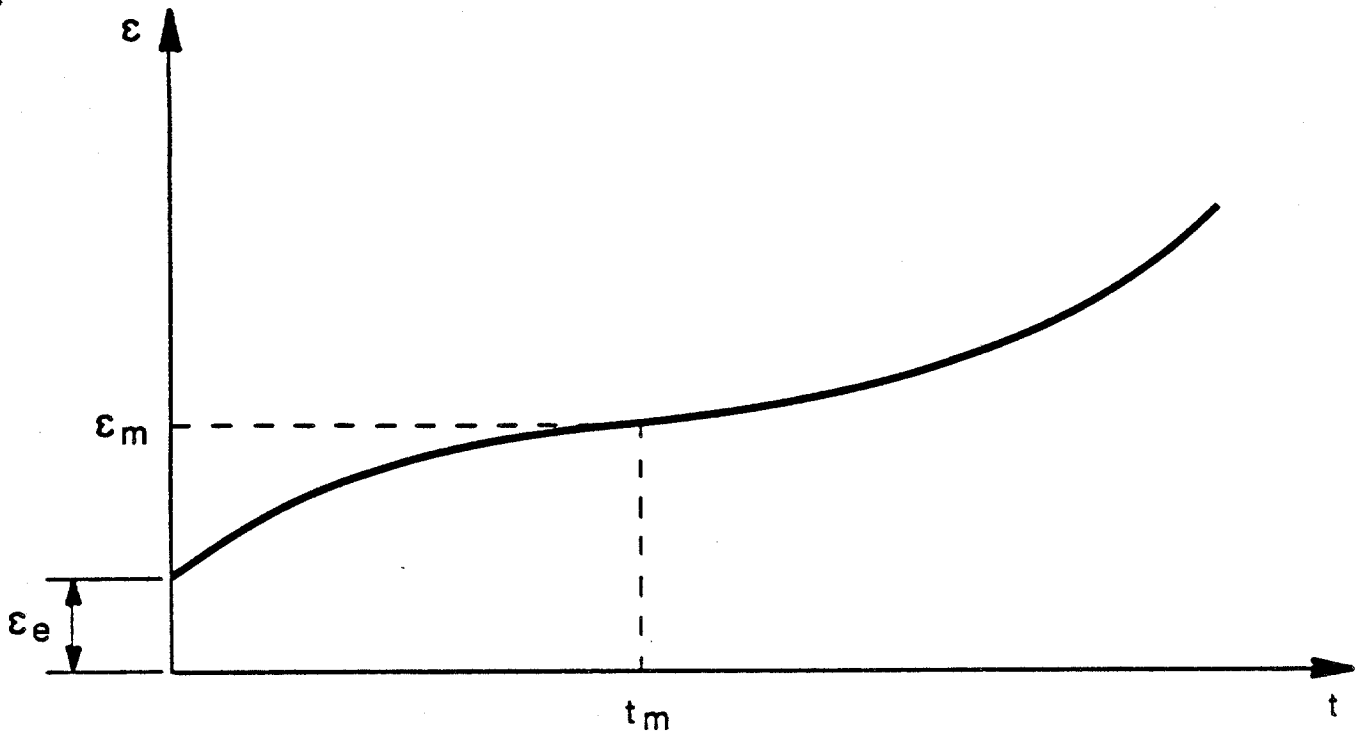


Fig. 1 - Idealized responses for uniaxial stress tests.

Consider now a family of constant strain rate curves. At constant strain rate  $\dot{\epsilon} = w$ , the typical stress-strain curve is shown in Figure 1(b). As  $w$  increases, the peak stress,  $\sigma_M$ , will increase and the corresponding strain,  $\epsilon_M$ , will decrease or remain approximately constant. From these observations, it is reasonable to assume that a family of constant strain rate curves will not intersect in at least the small strain ranges. Thus, for each strain,  $\epsilon$ , in this range, the stress increases with  $w$  and there exists a monotonic  $\bar{\sigma} - w$  relation which can be inverted:

$$\dot{\epsilon} = w = \text{constant}: \quad \bar{\sigma} = G(w, \epsilon), \quad w = W(\bar{\sigma}, \epsilon) \quad (6)$$

Applying the chain rule,  $\dot{\bar{\sigma}}$  can be rewritten as,

$$\dot{\bar{\sigma}} = \frac{\partial \bar{\sigma}}{\partial t} = \frac{\partial \bar{\sigma}}{\partial \epsilon} \dot{\epsilon} = \frac{\partial G}{\partial \epsilon} w. \quad (7)$$

Substituting for  $\dot{\bar{\sigma}}$  and  $\dot{\epsilon}$  in equation (2) and solving for  $\frac{\partial G}{\partial \epsilon}$ , we find:

$$\begin{aligned} \frac{\partial G}{\partial \epsilon} = Y(\bar{\sigma}, \epsilon) &= \left[ \frac{3\hat{\phi}}{2(1-\epsilon)^2\hat{\psi}} + \frac{2\bar{\sigma}}{(1-\epsilon)} \right] \left( 1 - \frac{F}{W} \right). \\ &= \hat{Y}(\bar{\sigma}, \epsilon) \left( 1 - \frac{F}{W} \right) \end{aligned} \quad (8)$$

The function  $Y(\bar{\sigma}, \epsilon)$  measures the stress-strain gradient of the constant strain rate response and represents a generalized Young's modulus. The function pair  $Y(\bar{\sigma}, \epsilon)$  and  $W(\bar{\sigma}, \epsilon)$  are two data functions which can be determined from a family of constant strain rate tests.

The three data functions  $Y$ ,  $W$ , and  $F$  are not sufficient to determine the three response functions  $\hat{\phi}$ ,  $\hat{\omega}$ , and  $\hat{\psi}$  since the constant load and constant strain rate test configurations only provide two independent relations given by equations (5) and (8). Morland<sup>2</sup> investigates the possibility of other uniaxial test configurations, such as constant load rate and constant displacement tests, providing a third independent relation. His results show that only two relations can be independent because equation (2) can be expressed in a form involving only two combinations of the coefficients, namely

$$\dot{\bar{\sigma}} = \hat{Y}(\bar{\sigma}, \epsilon)\dot{\epsilon} - L(\bar{\sigma}, \epsilon), \quad (9)$$

where  $\bar{L}(\sigma, \epsilon)$  is the data function obtained from a family of constant displacement tests. Morland concludes that any prescribed uniaxial stress history can only give relations involving combinations of  $\hat{Y}(\bar{\sigma}, \epsilon)$  and  $L(\bar{\sigma}, \epsilon)$ . Consequently, two-dimensional data are required to construct a uniaxial stress reduction of the tensor relation in (1). However, certain assumptions about the functional dependence of the response functions can permit the construction of one-dimensional stress models from one-dimensional data alone. Morland<sup>2</sup> describes the assumptions necessary to construct three of these so-called "reduced" models. It will be seen later that these reduced models are unsatisfactory.

#### LABORATORY TEST DATA

The first step in testing the applicability of the one-dimensional model given in equation (2) is to construct the data functions from laboratory test data. The test results from the Phase I experimental program show much scatter due to the large variations of ice types and physical properties of multiyear ice samples. The Phase I constant strain rate tests were conducted at two temperatures and two strain rates on samples taken from multiyear pressure ridges. Each test condition consisted of at least 40 tests. The Phase I constant load tests were a limited scope study on multiyear floe ice to develop test techniques for subsequent phases. These tests were conducted at two loads and two temperatures. Each test condition consisted of only two tests, and the results had in some cases differences of over an order of magnitude. Given the scatter in the data, the different ice type for each test type, the limited number of test conditions for each test type, and the small sample population for the constant load tests, the Phase I data set was not judged to be suitable for testing a new constitutive model.

The ideal data set for constructing the uniaxial data functions should consist of test samples which have consistent physical properties and test results from a large number of constant loads and constant strain rates. The data set which best fits these criteria is the data set obtained by Mellor and Cole.<sup>4</sup> Their tests were conducted on fine-grained isotropic ice under uniaxial compression at  $-5^{\circ}\text{C}$ . The applied stresses for the 24 constant

load tests ranged from 116 psi to 550 psi. The strain rates for the 26 constant strain rate tests ranged from  $10^{-7}$ /sec to  $10^{-3}$ /sec.

Four constant load tests and four constant strain rate tests were chosen from the entire Mellor and Cole data set to construct the data functions. The four constant load tests were chosen to divide the range of loads into approximately equal intervals. The minimum strain rates for the constant load tests ranged from  $1 \times 10^{-7}$ /sec to  $2.64 \times 10^{-5}$ /sec. Since two of the data functions correspond to typical strain rates of the two test types, the four chosen constant strain rate tests were restricted to this strain rate range to ensure an order of magnitude correspondence of strain rates between the two test types. If the resulting one-dimensional model shows merit in this restricted strain rate range, then the extension into larger ranges can be investigated later. Once the particular tests were chosen for each test type, exponential functions were fitted to each test to facilitate data manipulation. The procedures for each test type are discussed in the following.

#### Constant Load Tests

The typical strain, time response for ice under constant load test conditions can be approximated by an expression of the form,

$$\epsilon(t) = \epsilon_0 + \epsilon_1 e^{-t/t_1} + \epsilon_2 e^{-t/t_2} . \quad (10)$$

The constants  $\epsilon_0$ ,  $\epsilon_1$ ,  $\epsilon_2$ ,  $t_1$ , and  $t_2$  are determined by requiring that the key features of the observed response be matched exactly. In our case these are the elastic jump at  $t = 0$  and the minimum strain rate. Explicitly these requirements are:

1.  $\epsilon(0) = \epsilon_e$ ,
  2.  $\epsilon(t_m) = \epsilon_m$ ,
  3.  $\dot{\epsilon}(t_m) = \dot{\epsilon}_m$ ,
  4.  $\dot{\epsilon}(t_m) = 0$ ,
  5.  $\epsilon(t_\infty) = \epsilon_\infty$ .
- (11)

Here  $\epsilon_e$  denotes the elastic strain jump at  $t = 0$ ,  $(t_m, \epsilon_m)$  defines the point at which minimum strain rate occurs,  $\dot{\epsilon}_m$  is the measured minimum strain rate, and  $(t_{\infty}, \epsilon_{\infty})$  is a point beyond  $(t_m, \epsilon_m)$ . Condition (5) provides the fifth condition necessary to determine the five constants and insures that the measured response at large strains is well matched.

The specific constant load tests chosen from the Mellor and Cole data set are listed in Table 1 along with the data points used to calculate the constants for the approximating functions. The elastic jumps in Table 1 are not actual data points but are instead calculated by dividing the applied stress by the Young's Modulus. The Young's Modulus is determined by looking at the apparent initial tangent moduli of the constant strain rate tests and selecting a typical value. The value chosen for Young's Modulus is  $4.64 \times 10^{-5}$  psi.

Figure 2 illustrates a typical fit of the functional form given by equation (10) to the experimental data. When solving the nonlinear system given by equations (11), it is easier to pick good initial guesses for the solution by scaling the data with respect to  $(t_m, \epsilon_m)$ . The coordinate axes in Figure 2 are the scaled axes. Once a solution for the scaled constants is obtained, those values are unscaled. The unscaled solutions for the constants are listed for each test in Table 2. Figure 3 illustrates plots of all four fitted curves and represents the family of constant load tests to be used in the construction of the data functions.

#### Constant Strain Rate Tests

The typical force-time record for ice under constant strain rate test conditions can be approximated by an expression of the form,

$$f(t) = f_0 + f_1 e^{t/t_1} + f_2 e^{t/t_2} + f_3 e^{t/t_3}. \quad (12)$$

Although a constant plus two exponential terms is sufficient to describe the general shape of the force-time record, the additional exponential term provides a better fit for the post peak response. Values for  $t_1$  and  $t_2$  are assumed and values for  $f_0$ ,  $f_1$ ,  $f_2$ ,  $f_3$ , and  $t_3$  are calculated by requiring,

Table 1  
CONSTANT LOAD TESTS FROM MELLOR AND COLE USED TO GENERATE DATA FUNCTIONS

Test	Load (lb)	Stress (psi)	$\epsilon_e$ in./in.	$t_m$ (sec)	$\epsilon_m$ (in./in.)	$\dot{\epsilon}_m$ (1/sec)	$t_\infty$ (sec)	$\epsilon_\infty$ (in./in.)
96 CL	364	115.9	.00025	$7.00 \times 10^4$	.01011	$1.02 \times 10^{-7}$	$3.36 \times 10^5$	.0626
100 CL	838	266.7	.00058	$4.40 \times 10^3$	.00657	$1.16 \times 10^{-6}$	$2.94 \times 10^4$	.0783
11 CL	1070	340.5	.00073	$2.20 \times 10^3$	.00960	$2.60 \times 10^{-6}$	$1.44 \times 10^4$	.1472
6 CL	1425	453.5	.00097	$8.00 \times 10^2$	.00850	$6.33 \times 10^{-6}$	$5.73 \times 10^3$	.1642

TEST NUMBER: CL6  
APPLIED LOAD = 1425 LBS

✱ EXPERIMENTAL DATA  
— FITTED CURVE

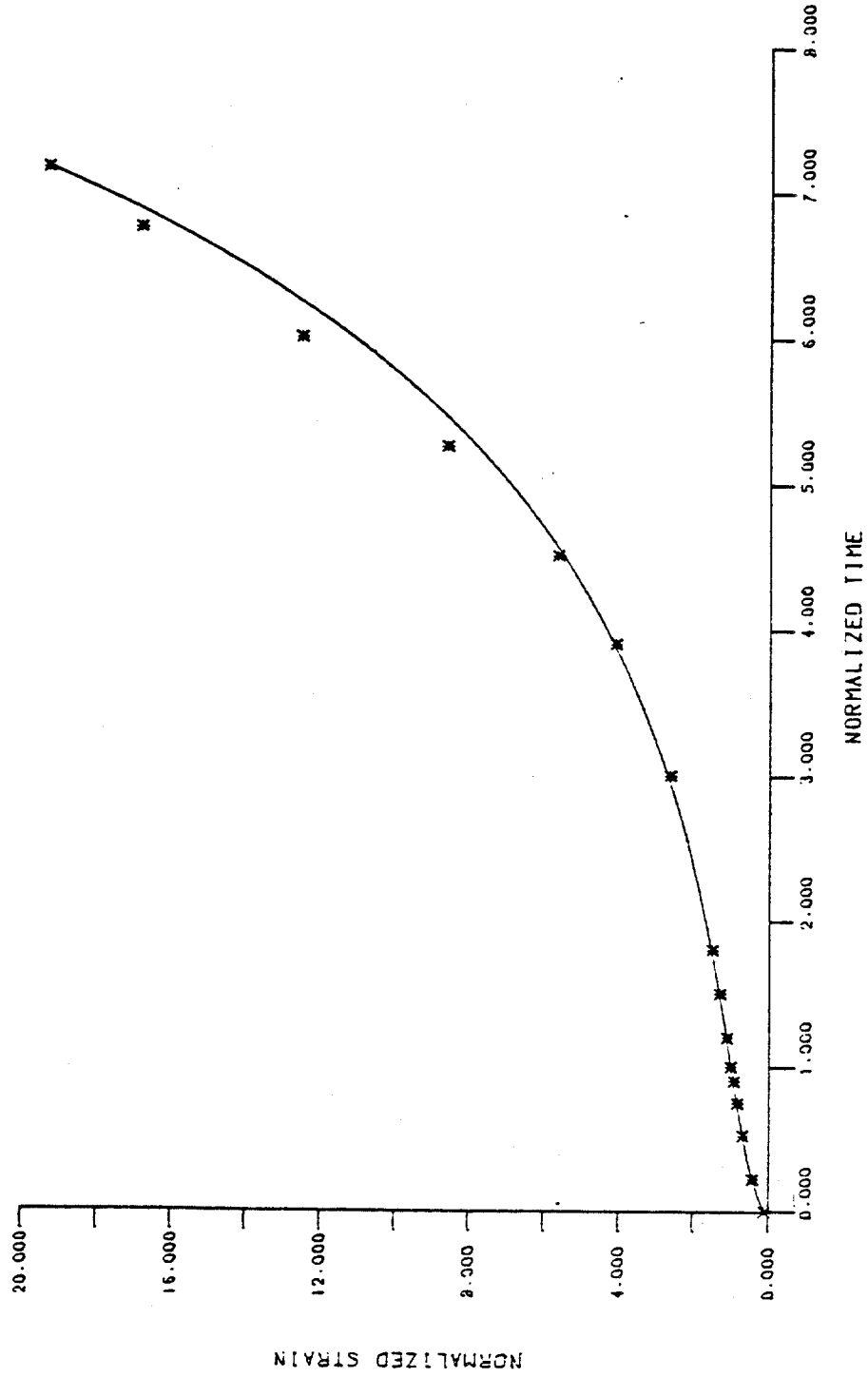


Fig. 2 - Typical fit of the assumed creep curve to experimental data.

Table 2  
CONSTANTS FOR THE APPROXIMATING FUNCTIONS OF THE CONSTANT LOAD TESTS  

$$\epsilon(t) = \epsilon_0 + \epsilon_1 e^{-t/t_1} + \epsilon_2 e^{-t/t_2}$$

Test Number	Stress (psi)	$\epsilon_0$ (in./in.)	$\epsilon_1$ (in./in.)	$\epsilon_2$ (in./in.)	$t_1$ (sec)	$t_2$ (sec)
1. 96 CL	115.8	$-4.12 \times 10^{-3}$	$-4.71 \times 10^{-3}$	$9.07 \times 10^{-3}$	$-4.02 \times 10^4$	$1.67 \times 10^5$
2. 100 CL	266.7	$-6.66 \times 10^{-3}$	$-2.62 \times 10^{-3}$	$9.85 \times 10^{-3}$	$-2.24 \times 10^3$	$1.36 \times 10^4$
3. 11 CL	340.5	$-3.55 \times 10^{-4}$	$-5.23 \times 10^{-3}$	$6.32 \times 10^{-3}$	$-7.41 \times 10^2$	$4.57 \times 10^3$
4. 6 CL	453.0	$-5.87 \times 10^{-4}$	$-4.30 \times 10^{-3}$	$5.87 \times 10^{-3}$	$-2.82 \times 10^3$	$1.72 \times 10^3$

# CONSTANT LOAD TESTS (MELLOR & COLE DATA)

- 364 LBS
- 837 LBS
- ▲ 1070 LBS
- ✱ 1425 LBS

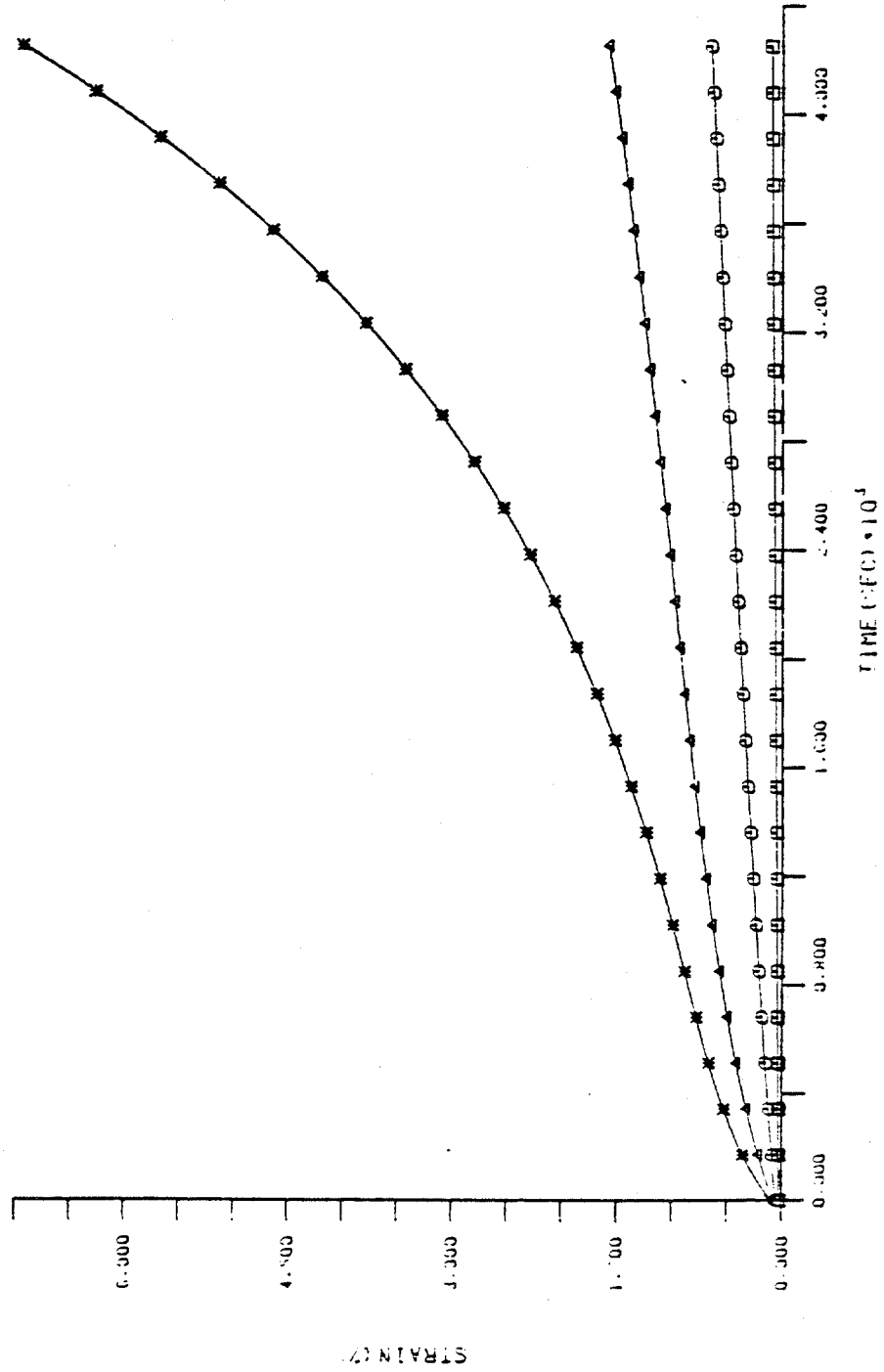


Fig. 3 - Family of creep curves used to construct the data functions.

1.  $f(0) = 0,$
2.  $\dot{f}(0) = \dot{F}_i,$
3.  $f(t_m) = f_m,$  (13)
4.  $\dot{f}(t_m) = 0,$
5.  $f(t_\infty) = f_\infty .$

Here  $\dot{F}_i$  is the initial slope of the force time record,  $(t_m, f_m)$  is the peak of the force time record, and  $(t_\infty, f_\infty)$  is some point beyond the peak value. The specific constant strain rate test chosen from the Mellor and Cole data set is listed in Table 3 along with the data points used to calculate the constants.

Figure 4 illustrates a typical fit of the functional form given in equation (12) to the experimental data. The fitted curve and experimental data in this figure are normalized with respect to the point  $(t_m, f_m)$ . In Figure 4, the local maximum seen in the experimental points is a typical feature of the curves obtained by Mellor and Cole and represents the initial yield point of the material. The primary objective here is to obtain a family of stress-strain curves which exhibit an increase in strength with increasing strain rate and strain softening. Consequently, no attempt is made to include the initial yield point in the approximating functions.

The stress-strain curve for the experimental data is easily approximated by appropriately scaling equation (12). In developing the family of constant strain rate curves, it is assumed that the initial material response is elastic for each test. Thus, the initial slope of the force time curve is actually a calculated value obtained by multiplying the Young's modulus by the initial cross-sectional area of the test sample and the test strain rate. The value of Young's modulus is the same value (i.e., 464,000 psi) used to calculate the elastic jumps for the family of constant load tests.

The unscaled solutions for the constants of the functions describing the force time records are listed in Table 4. Table 5 contains the scaled constants which yield the corresponding stress-strain curves. The family of

Table 3

CONSTANT STRAIN RATE TESTS FROM MELLOR AND COLE  
USED TO GENERATE DATA FUNCTIONS

Test	$\dot{\epsilon}$ (1/sec)	$\dot{F}_i$ (lb/sec)	$t_M$ (sec)	$f_M$ (lb)	$t_\infty$ (sec)	$f_\infty$ (lb)
121 CD	$7.8 \times 10^{-7}$	1.137	16260	570	66660	430
123 CD	$2.25 \times 10^{-6}$	3.280	4650	933	15870	635
46 CD	$1.32 \times 10^{-5}$	19.240	660	1470	2160	1120
31 CD	$5.14 \times 10^{-5}$	74.930	179	1859	1167	1271

TEST NUMBER: CD121  
STRAIN RATE =  $(7.8E-7)$ /SEC

■ EXPERIMENTAL DATA  
— FITTED CURVE

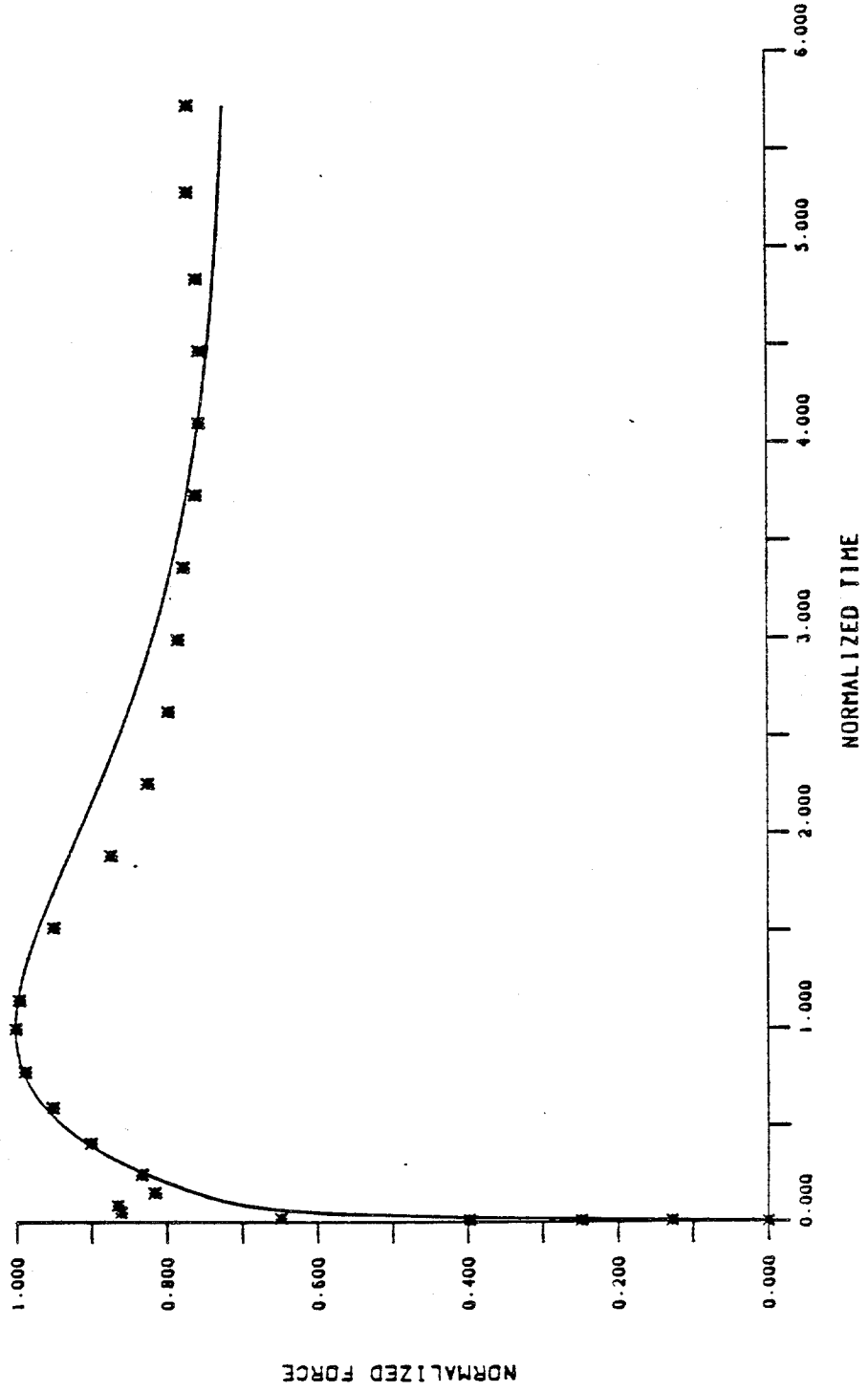


Fig. 4 - Typical fit of the assumed stress-strain curve to experimental data.

Table 4  
CONSTANTS FOR THE APPROXIMATING FUNCTIONS OF THE FORCE TIME CURVES

$$f(t) = f_0 + f_1 e^{-t/\tau_1} + f_2 e^{-t/\tau_2} + f_3 e^{-t/\tau_3}$$

Test	$\dot{\epsilon}$ (1/sec)	$f_0$ (lb)	$f_1$ (lb)	$f_2$ (lb)	$f_3$ (lb)	$\tau_1$ (sec)	$\tau_2$ (sec)	$\tau_3$ (sec)
121 CD	$7.8 \times 10^{-7}$	$4.05 \times 10^2$	$3.00 \times 10^3$	$-3.04 \times 10^3$	$-3.62 \times 10^2$	$-1.63 \times 10^4$	$-1.38 \times 10^4$	$-3.28 \times 10^2$
123 CD	$2.25 \times 10^{-6}$	$5.42 \times 10^2$	$4.25 \times 10^3$	$-4.45 \times 10^3$	$-3.43 \times 10^2$	$-4.65 \times 10^3$	$-3.49 \times 10^3$	$1.18 \times 10^2$
46 CD	$1.32 \times 10^{-5}$	$9.92 \times 10^2$	$5.19 \times 10^3$	$-5.43 \times 10^3$	$-7.50 \times 10^2$	$-6.60 \times 10^2$	$-4.95 \times 10^2$	$-4.65 \times 10^1$
31 CD	$5.14 \times 10^{-5}$	$1.26 \times 10^3$	$1.08 \times 10^4$	$-1.10 \times 10^4$	$-1.11 \times 10^3$	$-1.79 \times 10^2$	$-1.52 \times 10^2$	$-1.75 \times 10^1$

Table 5  
CONSTANTS FOR THE APPROXIMATING FUNCTIONS OF THE STRESS-STRAIN CURVES

$$\sigma(\epsilon) = \sigma_0 + \sigma_1 e^{\epsilon/\epsilon_1} + \sigma_2 e^{\epsilon/\epsilon_2} + \sigma_3 e^{\epsilon/\epsilon_3}$$

Test	$\dot{\epsilon}$ (1/sec)	$\sigma_0$ (psi)	$\sigma_1$ (psi)	$\sigma_2$ (psi)	$\sigma_3$ (psi)	$\epsilon_1$ (in./in.)	$\epsilon_2$ (in./in.)	$\epsilon_3$ (in./in.)
121 CD	$7.8 \times 10^{-7}$	$1.29 \times 10^2$	$9.55 \times 10^2$	$-9.68 \times 10^2$	$-1.15 \times 10^2$	$-1.27 \times 10^{-2}$	$-1.08 \times 10^{-2}$	$-2.56 \times 10^{-4}$
123 CD	$2.25 \times 10^{-6}$	$1.73 \times 10^2$	$1.35 \times 10^3$	$-1.42 \times 10^3$	$-1.09 \times 10^2$	$-1.05 \times 10^{-2}$	$-7.85 \times 10^{-3}$	$-2.66 \times 10^{-4}$
46 CD	$1.32 \times 10^{-5}$	$3.16 \times 10^2$	$1.65 \times 10^3$	$-1.73 \times 10^3$	$-2.39 \times 10^2$	$-8.71 \times 10^{-3}$	$-6.53 \times 10^{-3}$	$-6.14 \times 10^{-4}$
31 CD	$5.14 \times 10^{-5}$	$4.01 \times 10^2$	$3.44 \times 10^3$	$-3.50 \times 10^3$	$-3.53 \times 10^2$	$-9.20 \times 10^{-3}$	$-7.81 \times 10^{-3}$	$-9.00 \times 10^{-4}$

stress-strain curves which are to be used to construct the data functions are shown in Figure 5.

### CONSTRUCTION OF DATA FUNCTIONS

Before constructing the data functions, the approximating functions for each constant load test and each constant strain rate test are made non-dimensional by dividing each time, strain, and stress quantity by scale factors. The time scale,  $t_s = 720$  sec, is the time to minimum strain rate of the constant load test with the largest applied load, the strain scale,  $\epsilon_s = 0.008$ , is the strain at  $t_s$ , and the stress scale,  $\sigma_s = 592$  psi, is the maximum stress of the constant strain rate test with the highest strain rate.

The three data functions,  $F$ ,  $W$ , and  $Y$  constructed from the dimensionless equations are functions of the normalized stress,  $s = \sigma/\sigma_s$ , and normalized strain,  $e = \epsilon/\epsilon_s$ . The data functions will be represented as surfaces defined over the stress-strain plane. Attention is restricted to the points  $(s,e)$  in the domain defined by  $0 < s \leq 1$  and  $0 < e \leq 4$ . It will be seen later that the data functions obtained from each test type will be restricted to a subset of points in this domain.

#### Constant Load Data Function

The family of constant load curves yields the data function  $F$  which describes the strain rate response of the material. The actual family of constant load tests to be used is shown in Figure 3 and for the sake of discussion, a schematic representation of those curves is shown with normalized axes in Figure 6.

We want to construct the function  $F$  defined over some stress-strain domain determined by the family of constant load test. Consider the family of curves in Figure 6 obtained by applying the constant stresses  $S_k$ ,  $k = 1,4$ . Clearly the stress will range between the lowest and highest applied stresses. In our case, this range is  $S_1 = .196 \leq s \leq .766 = S_4$ . For any constant load test, the lower bound on strain is the elastic jump defined by Hooke's law. All subsequent strains lie to the right of the elastic jump. Thus, all permissible  $(s,e)$  points associated with any constant load test lie in a restricted region to the right of the line  $s = \bar{Y}e$  where  $\bar{Y}$  is the normalized Young's modulus. In our case the lower bound on strain is  $E_l = S_1/\bar{Y} = .0313$  and we arbitrarily specify the upper bound to be  $E_u = 4.0$ . The resulting stress-strain domain for our family of constant load tests is illustrated in Figure 7 by the cross-hatched trapezoid.

# CONSTANT STRAIN RATE TESTS (MELLOR & COLE DATA)

- 7.4E-7/SEC
- 2.25E-6/SEC
- ▲ 1.32E-5/SEC
- 5.14E-5/SEC

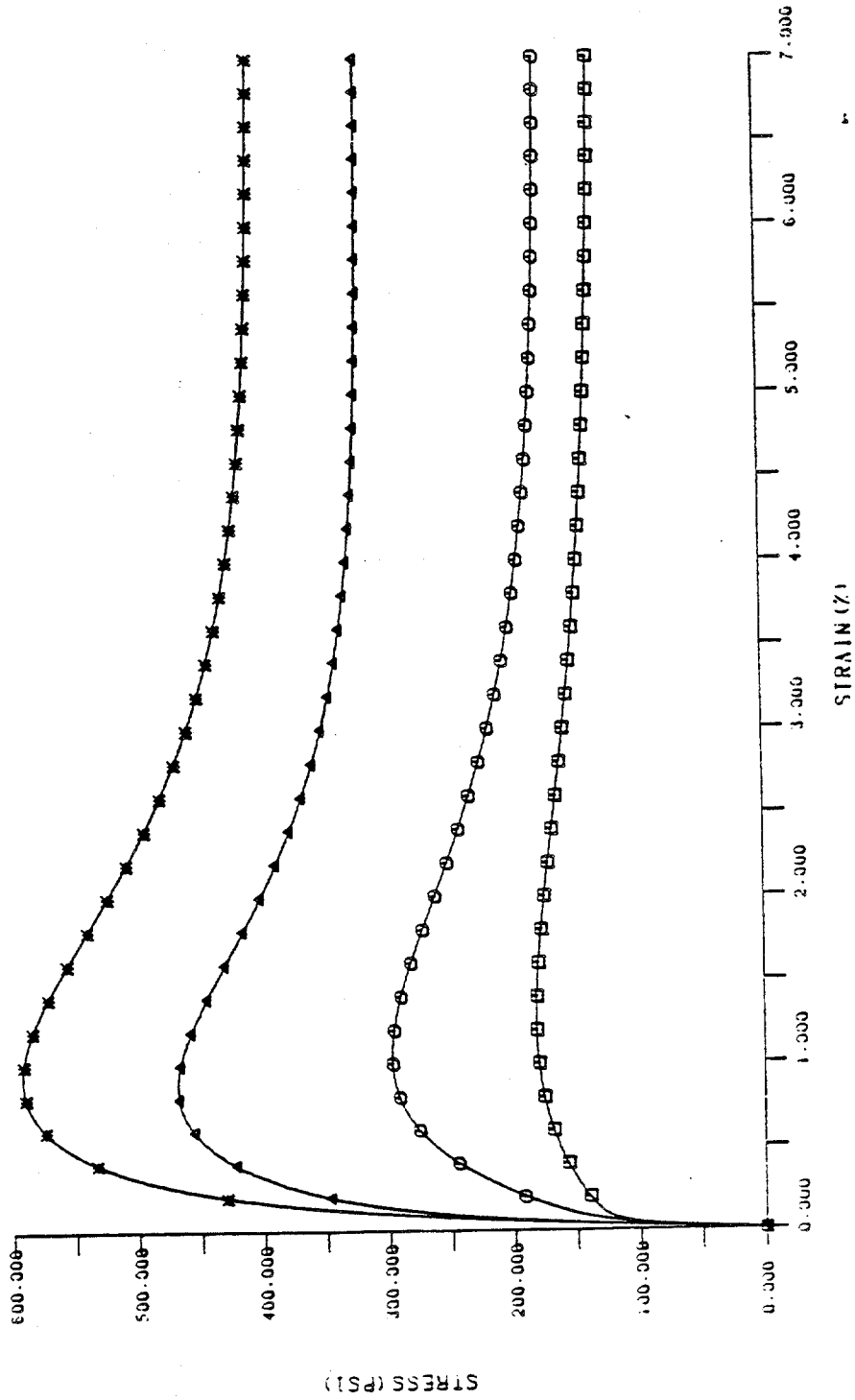


Fig. 5 - Family of stress-strain curves used to construct the data function.

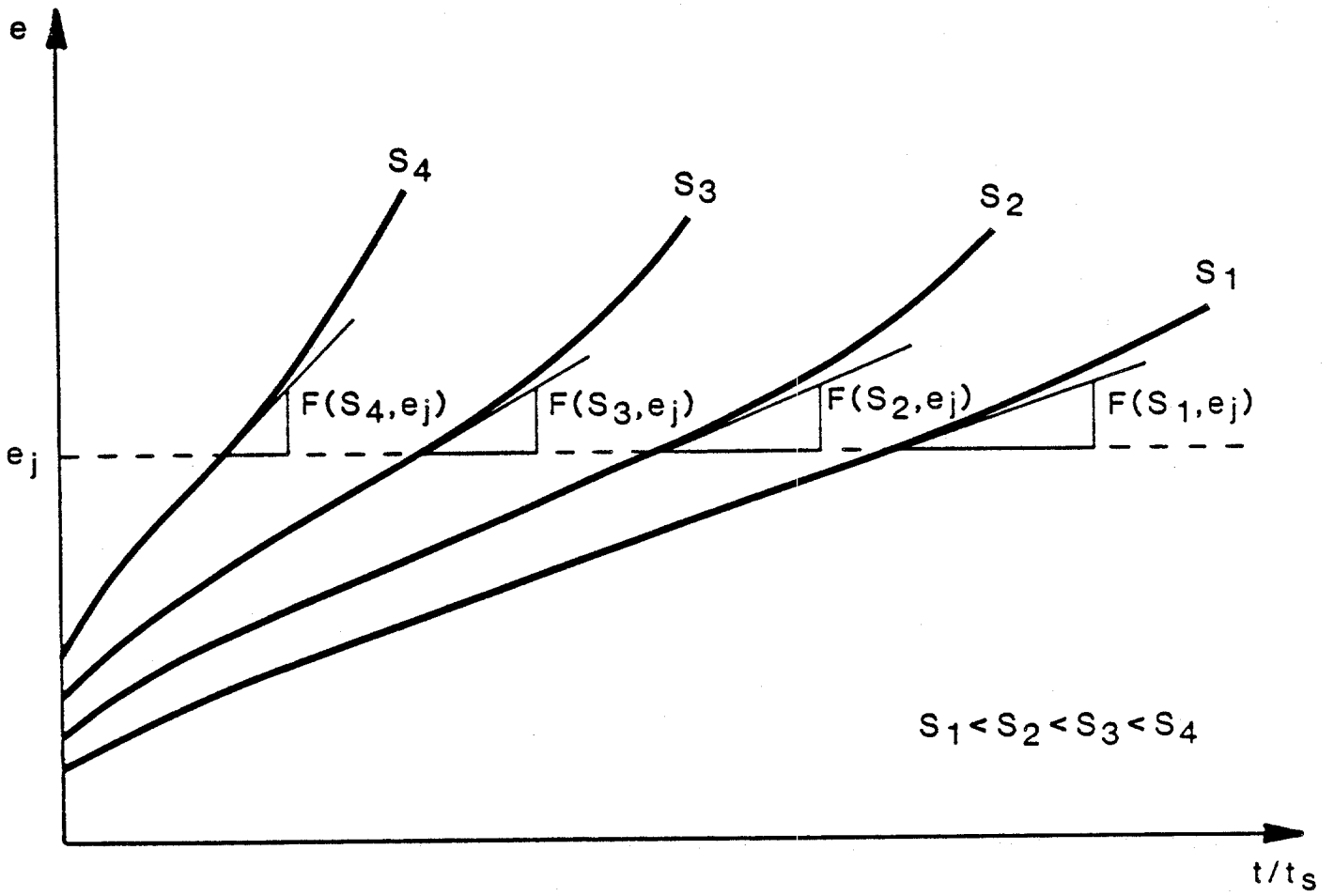


Fig. 6 - Calculation of the data function  $F$  from the constant load curves.

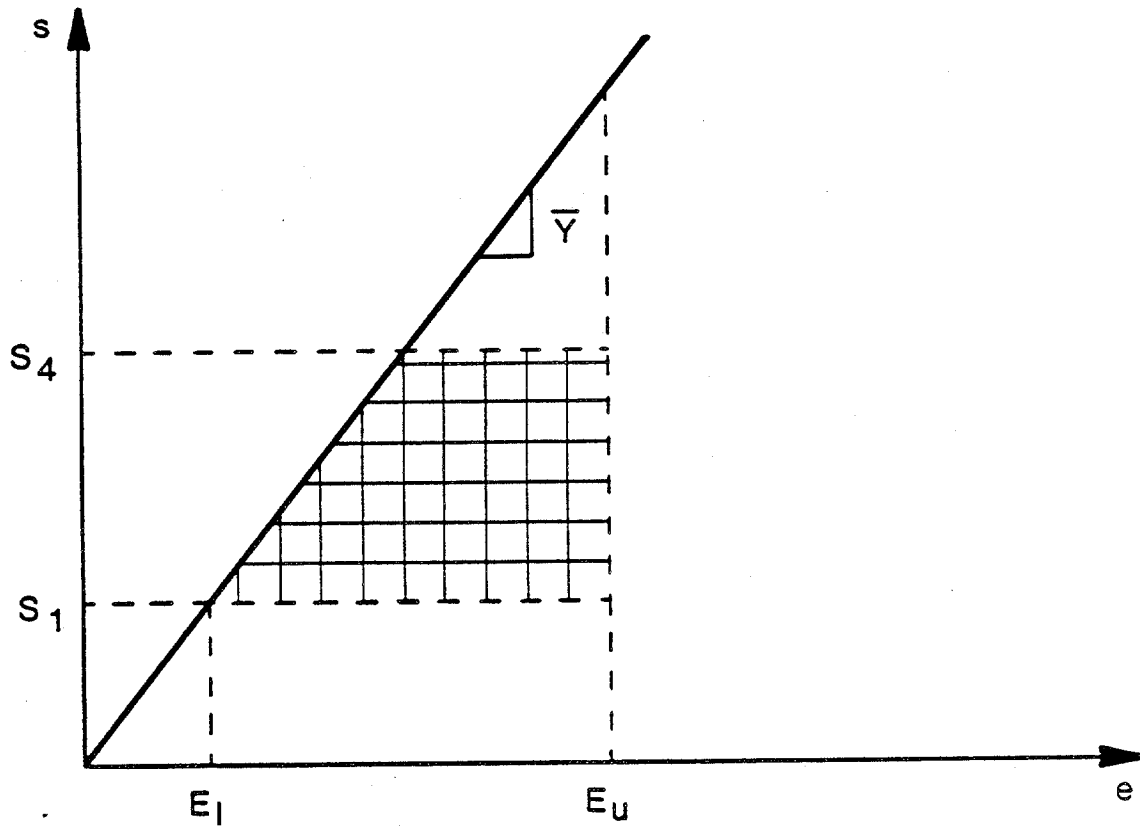


Fig. 7 - Stress-strain domain for constant load tests.

We want to evaluate the function  $F$  at any arbitrary set of points  $(s_i, e_j)$  defined by the partitions,  $S_1 \leq s_i \leq S_4$ ,  $i = 1, m$  and  $E_l \leq e_j \leq E_u$ ,  $j = 1, n$ . Consider the constant strain  $e_j$  shown in Figure 6. The function  $F$  can be evaluated by measuring the slope at the intersection of  $e_j$  and each constant load curve identified by the applied stress  $S_k$ . The ordered pairs  $(S_k, F(S_k, e_j))$  can then be mapped into the constant  $e_j$  plane as shown in Figure 8. The values of  $F(s_i, e_j)$  can then be evaluated by constructing an interpolating function between the mapped points. This procedure is repeated for each  $e_j$  until the function  $F(s_i, e_j)$  is defined at every point.

From Figure 6, we see that for a constant strain,  $e_j$ , the measured value of  $F$  increases with increasing  $S_i$ . The resulting mapping in the constant  $e_j$  plane should then be a monotonically increasing function as shown in Figure 8. An exponential function of the form  $F = a + be^s$  is chosen to evaluate  $F$  at all  $s_i$ . Two of the constants of this function are chosen to fit the endpoints  $F(S_1, e_j)$  and  $F(S_4, e_j)$  exactly and the third is chosen by minimizing the error from the intermediate points,  $F(S_2, e_j)$  and  $F(S_3, e_j)$ . The function  $F(s_i, e_j)$  is shown plotted in Figure 9, and Figures 10 and 11 show plots of  $F$  for planes of constant strain and stress, respectively.

#### Constant Strain Rate Data Functions

The family of constant strain rate curves yields the data functions  $W$  and  $Y$  which describe the material's strain rate and stress-strain gradient responses, respectively. The actual family of constant strain rate tests to be used in the construction of these functions is shown in Figure 5, and for the sake of discussion, a schematic representation of those curves is shown with normalized axes in Figure 12.

In constructing the functions which approximate the family of constant strain rate curves, we have assumed the initial response of the material to be elastic by requiring the initial slope for each curve to be equal to Young's modulus. Because of viscoelastic effects, the slopes of each curve will decrease from the initial value at rates dependent on the strain rate. Thus, for any constant strain rate test, all permissible stress-strain points will be in the region to the right of the line  $s = \bar{Y}e$ . As strain rate decreases, the departure from the initial Young's modulus will increase at faster rates. This, along with the observation that peak strength decreases with decreasing strain rate, guarantees that each stress-strain point to the

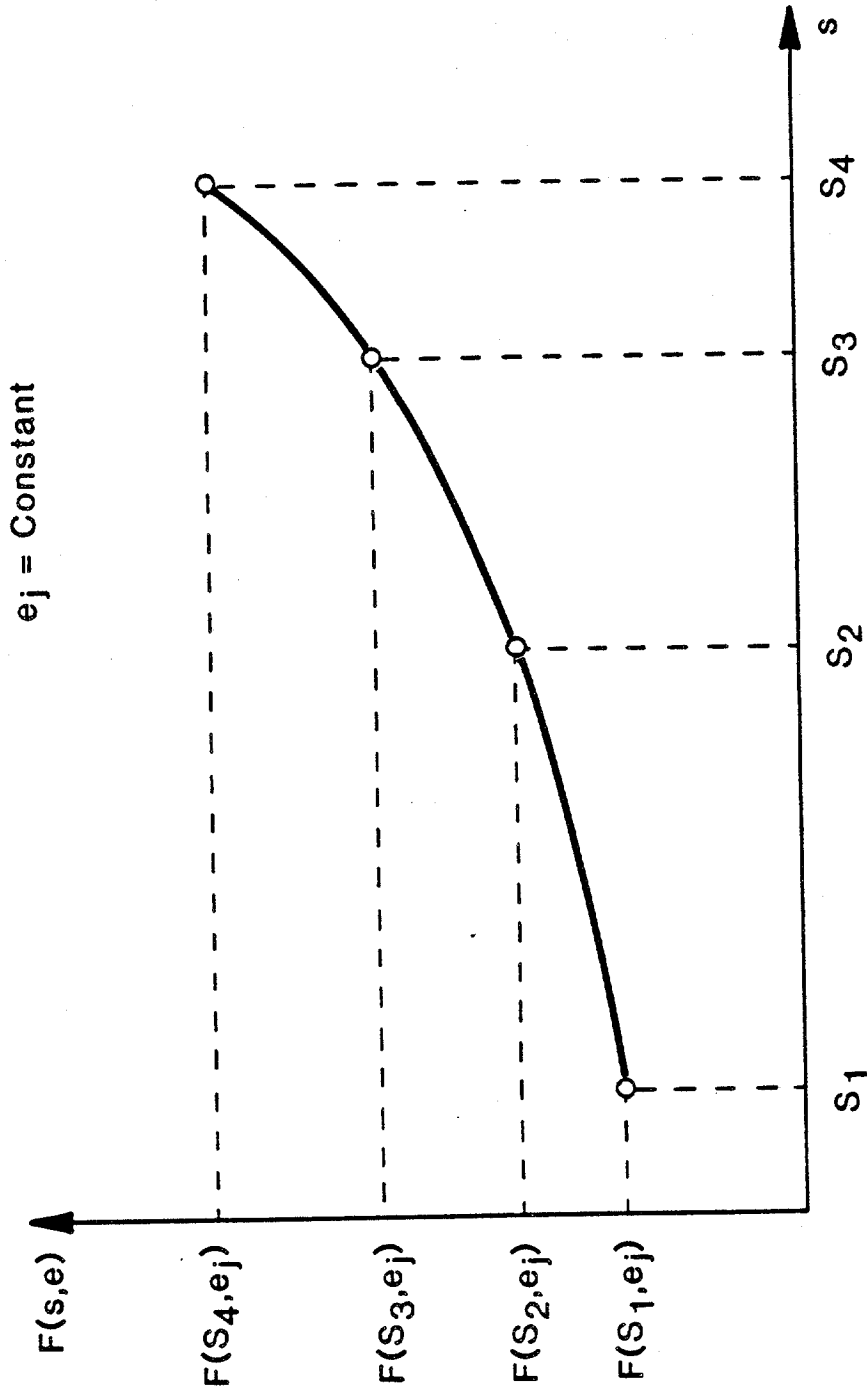


Fig. 8 - Mapping of the points  $F(S_k, e_j)$ ,  $k = 1,4$  into the  $e_j = \text{constant}$  plane.

# F DATA FUNCTION

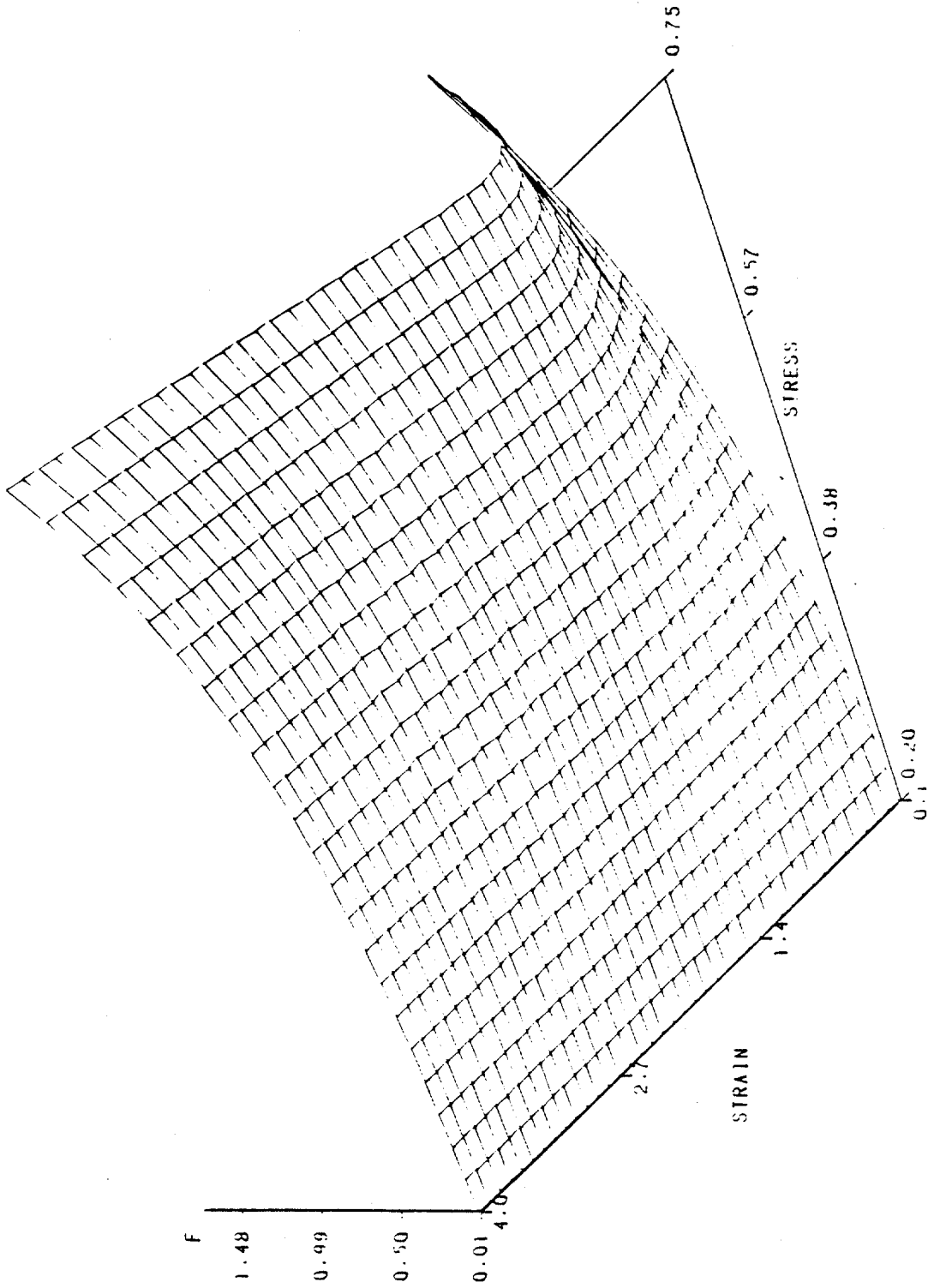


Fig. 9 - Three-dimensional representation of the F data function.

# F DATA FUNCTION CONSTANT STRAIN PLANES

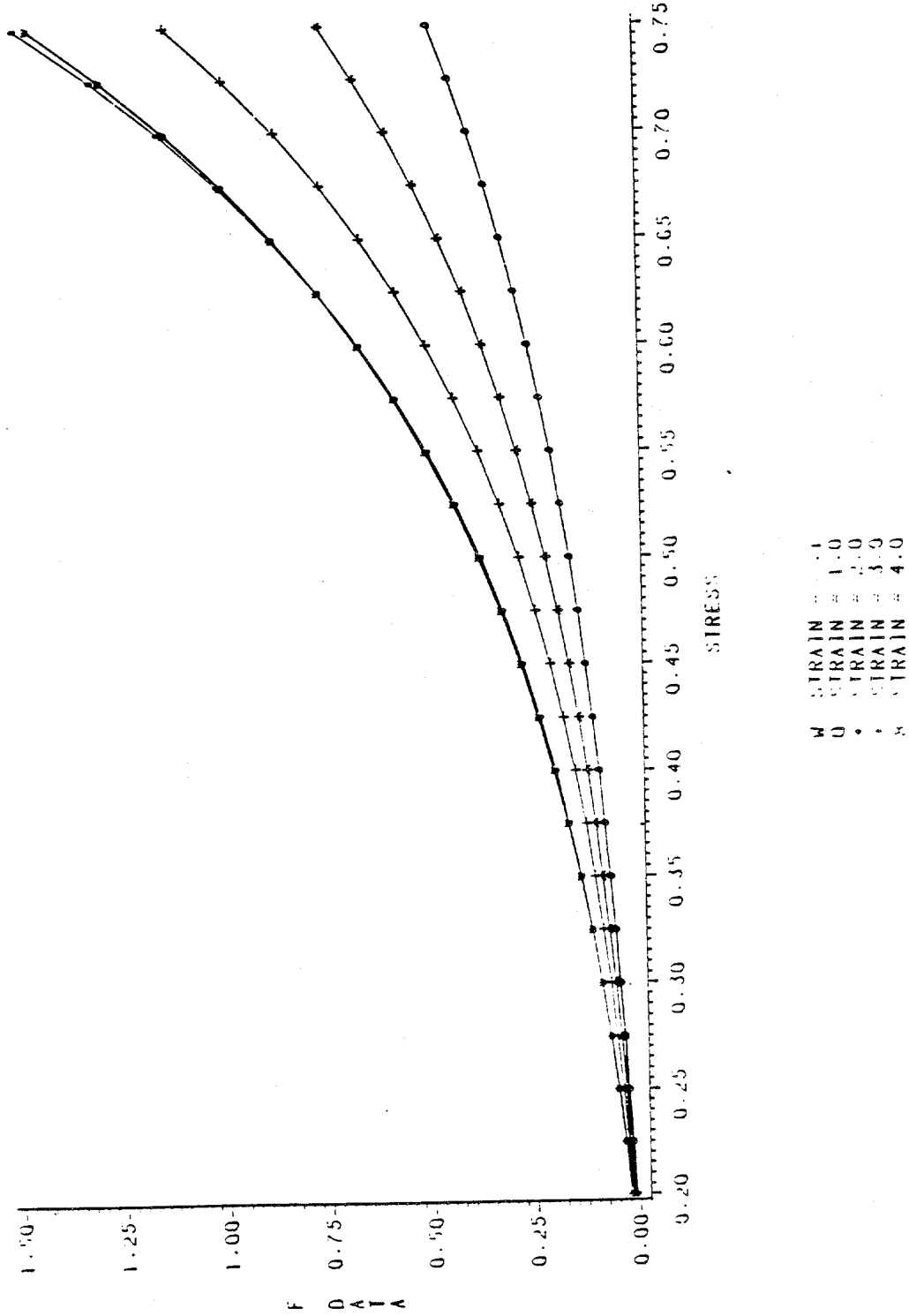


Fig. 10 - Planes of constant strain for the F data function.

# F DATA FUNCTION CONSTANT STRESS PLANES

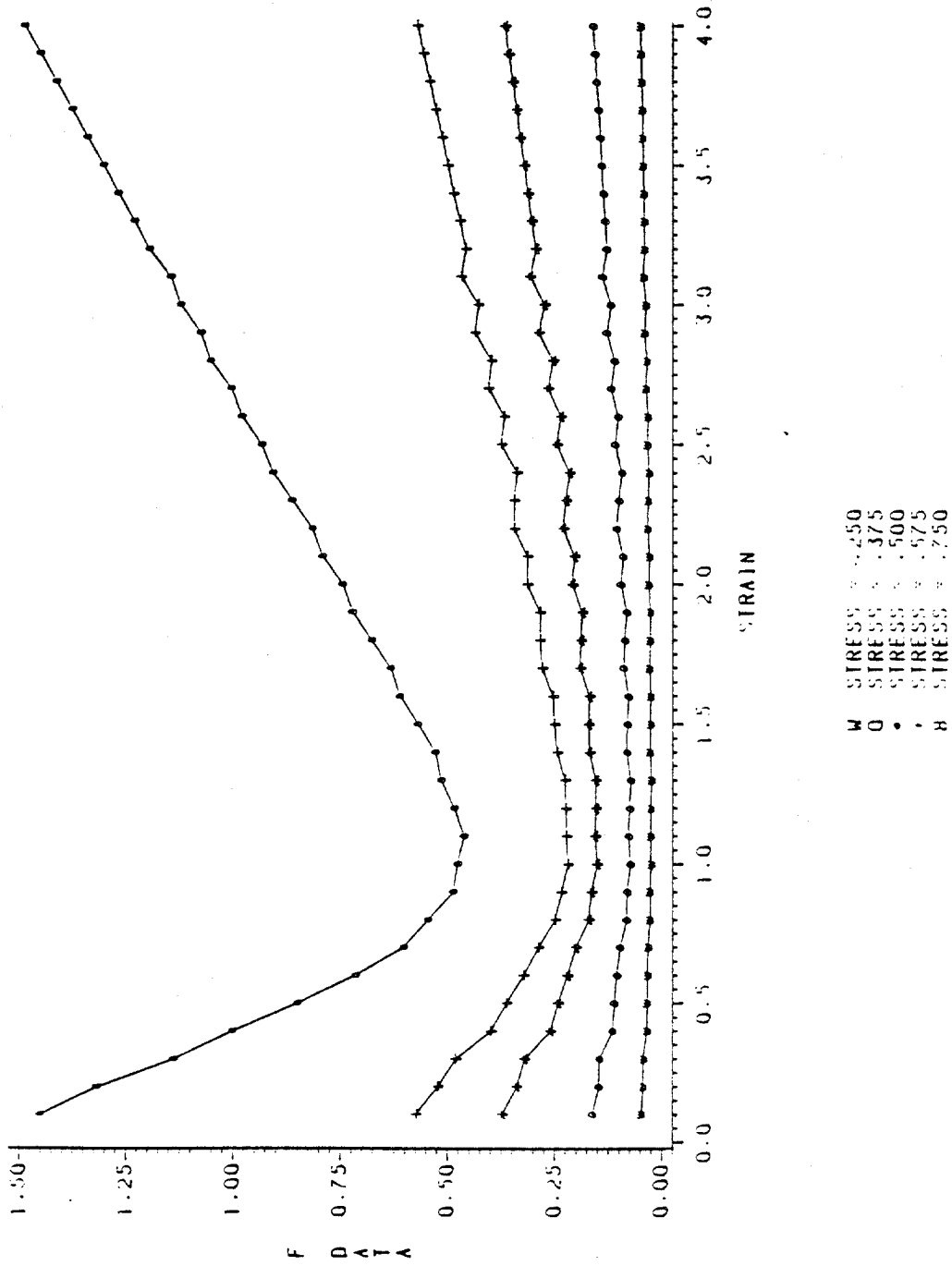


Fig. 11 - Planes of constant stress for the F data function.

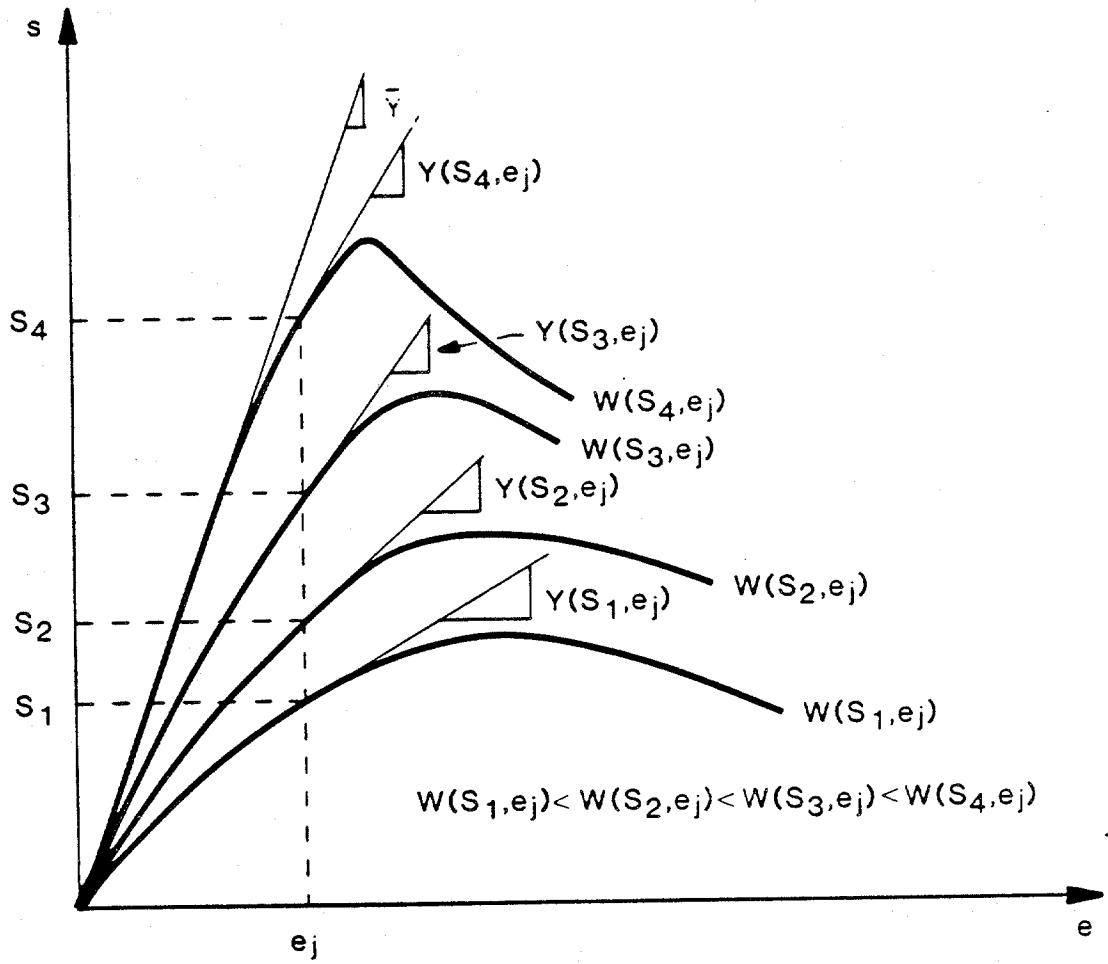


Fig. 12 - Calculation of the Y and W data functions from the constant strain rate curves.

right of  $s = \bar{Y}e$  corresponds to a single constant strain rate curve (at least at small strains).

We arbitrarily restrict strain to the interval,  $E_2 = 0 < e \leq 4.0 = E_u$ . The partially open interval at 0 will be discussed later. Consider a partition of this interval defined by  $E_2 < e_j \leq E_u$ ,  $j = 1, n$ . The constant strain  $e_j$ , shown in Figure 12, intersects each stress-strain curve. The intersections are defined by the stress values,  $S_k$ ,  $k = 1, 4$  where  $S_1 < S_2 < S_3 < S_4$ . Clearly for  $e_j = \text{constant}$  the stress domain is defined by  $S_1(e_j) \leq s \leq S_4(e_j)$ . Since this is true for any  $e_j$ , we see that in our case the stress-strain domain is further restricted to all points lying on and between the two curves with the highest and lowest strain rates, shown schematically in Figure 13.

At each intersection of  $e_j$ , the slope and strain rate of each stress-strain curve can be associated with each  $S_k$ . The ordered pairs  $(S_k, W(S_k, e_j))$  and  $(S_k, Y(S_k, e_j))$  can then be mapped into planes of constant  $e_j$  as shown in Figure 14. The functions  $W(s, e_j)$  and  $Y(s, e_j)$  can be evaluated for any  $s$  in  $S_1(e_j) \leq s \leq S_4(e_j)$  by choosing appropriate interpolating functions between the mapped points. Again, this procedure is repeated for each  $e_j$  until  $W$  and  $Y$  are defined everywhere.

From Figure 12 we see that the mapping of the points  $(S_k, W(S_k, e_j))$  must be a monotonically increasing function of  $S_k$  as shown in Figure 14a. Consequently, we choose an exponential function of the form  $W = a + be^{cs}$  to interpolate between the mapped points. The endpoints are again matched exactly and the intermediate points are fit in a least squares sense. Because of strain softening, the mapping of the points  $(S_k, Y(S_k, e_j))$  from Figure 12 may or may not be monotonic. Figure 14b illustrates a possible nonmonotonic mapping of these points. To allow for nonmonotonicity, cubic polynomials are chosen to interpolate between the mapped points. Continuity of the interpolating functions and their first derivatives are required at each intermediate mapped point.

Figure 15 is a three-dimensional plot of  $W(s, e)$  with Figures 16 and 17 illustrating traces of  $W$  in constant strain and stress planes, respectively. Figure 18 is a three-dimensional plot of  $Y(s, e)$  with constant strain and stress planes of  $Y$  illustrated in Figures 19 and 20, respectively.

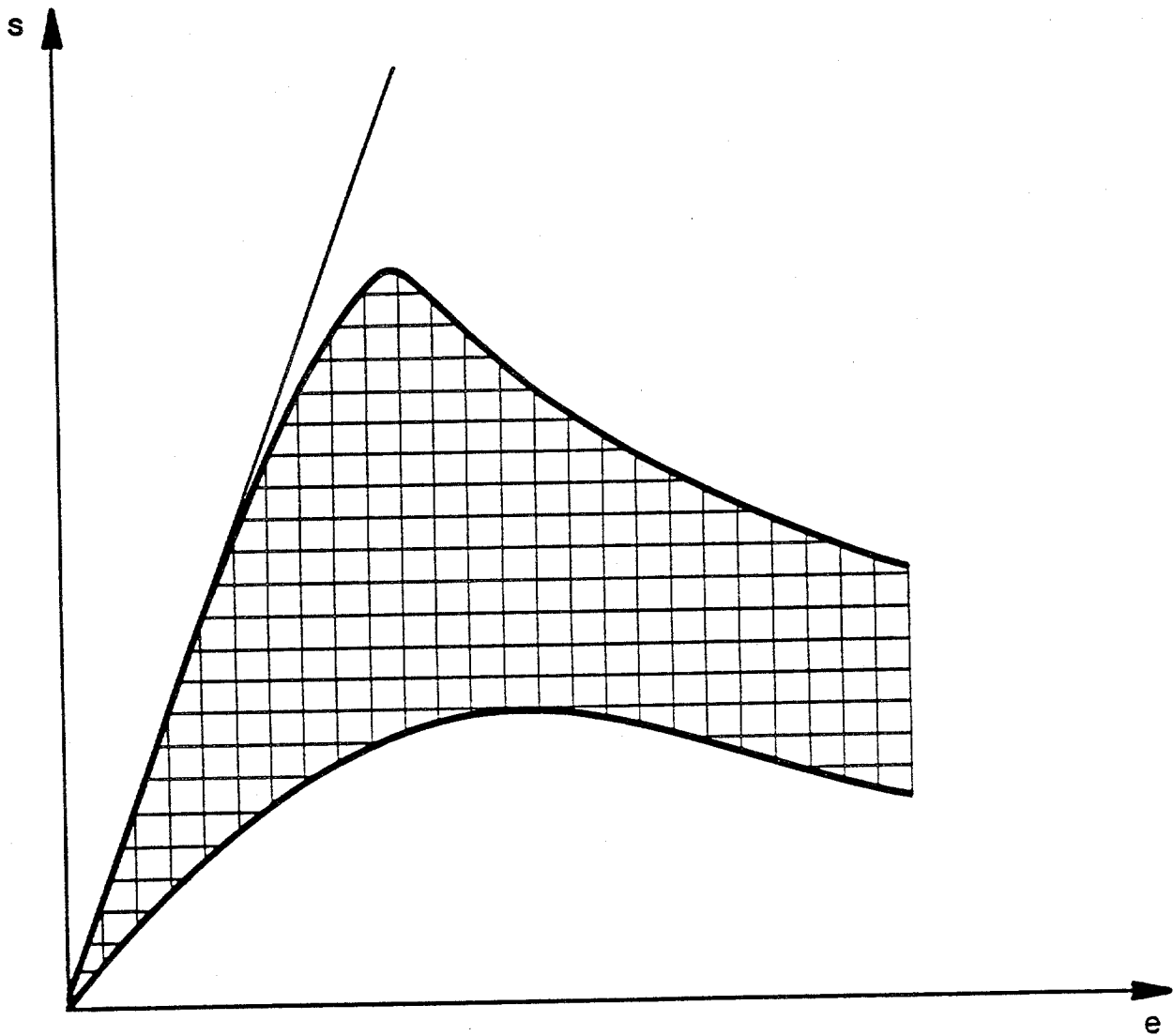


Fig. 13 - Stress-strain domain for W and Y data functions.

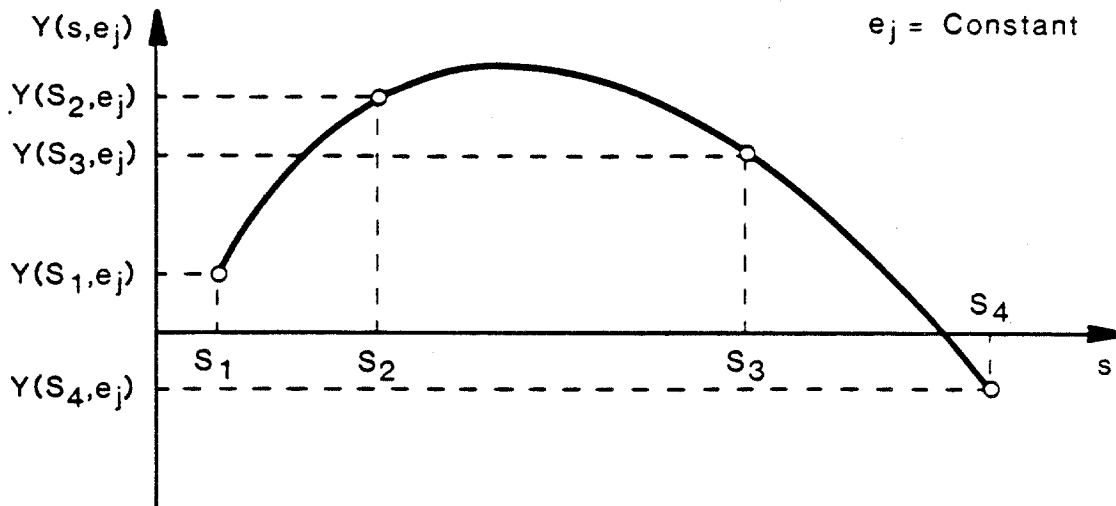
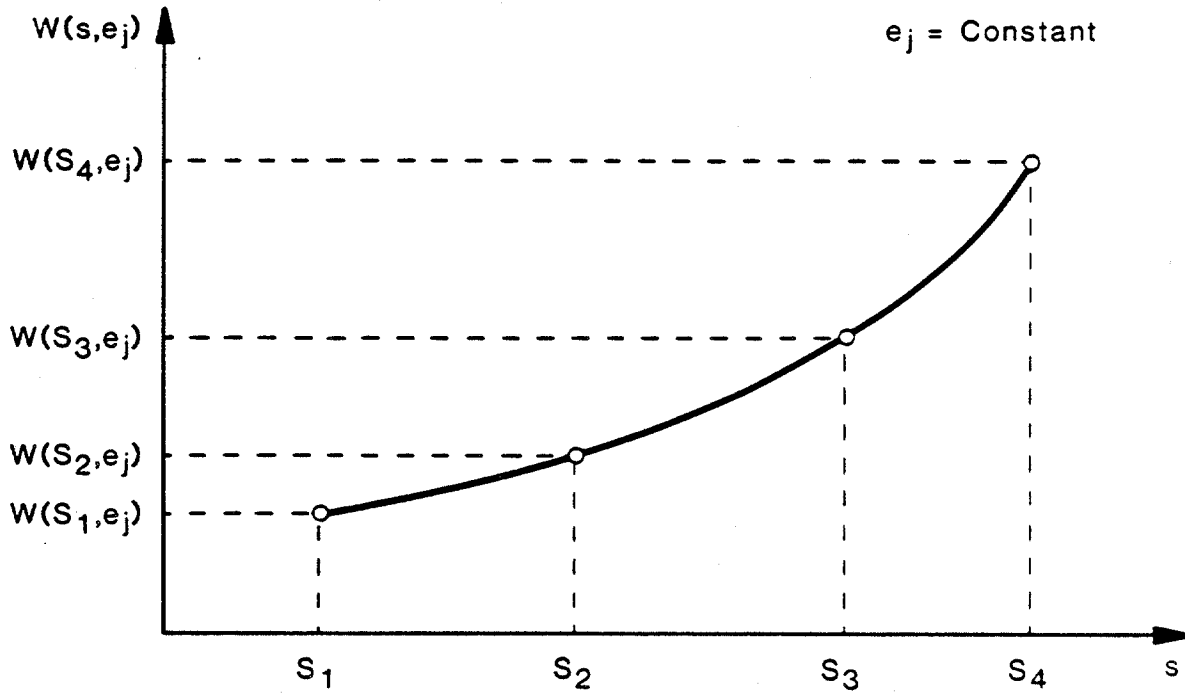


Fig. 14 - Mapping of the points  $W(S_k, e_j)$  and  $Y(S_k, e_j)$   $k = 1, 4$  into the  $e_j = \text{constant}$  plane.

# W DATA FUNCTION

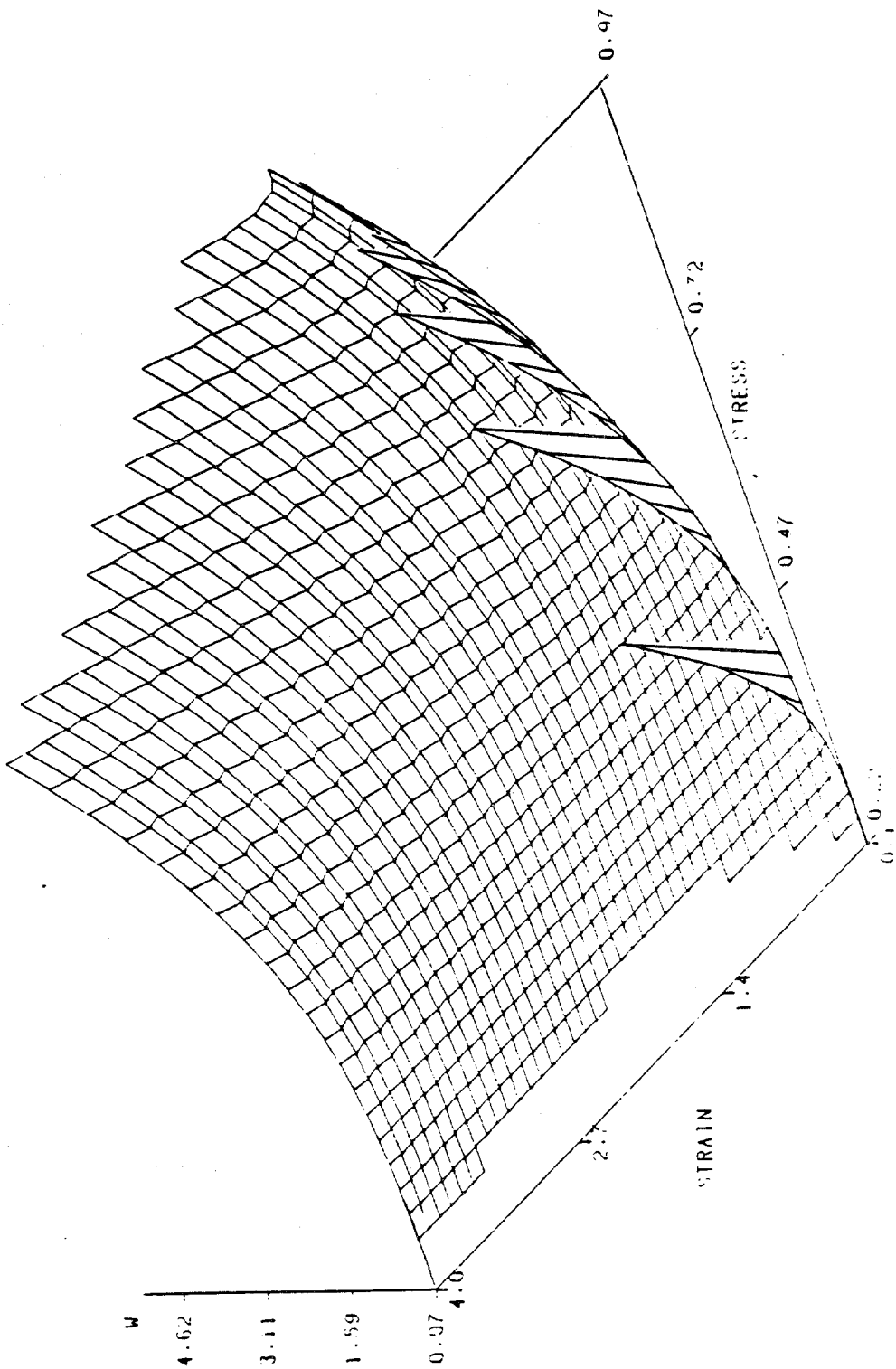


Fig. 15 - Three-dimensional representation of the W data function.

W DATA FUNCTION  
CONSTANT STRAIN PLANES

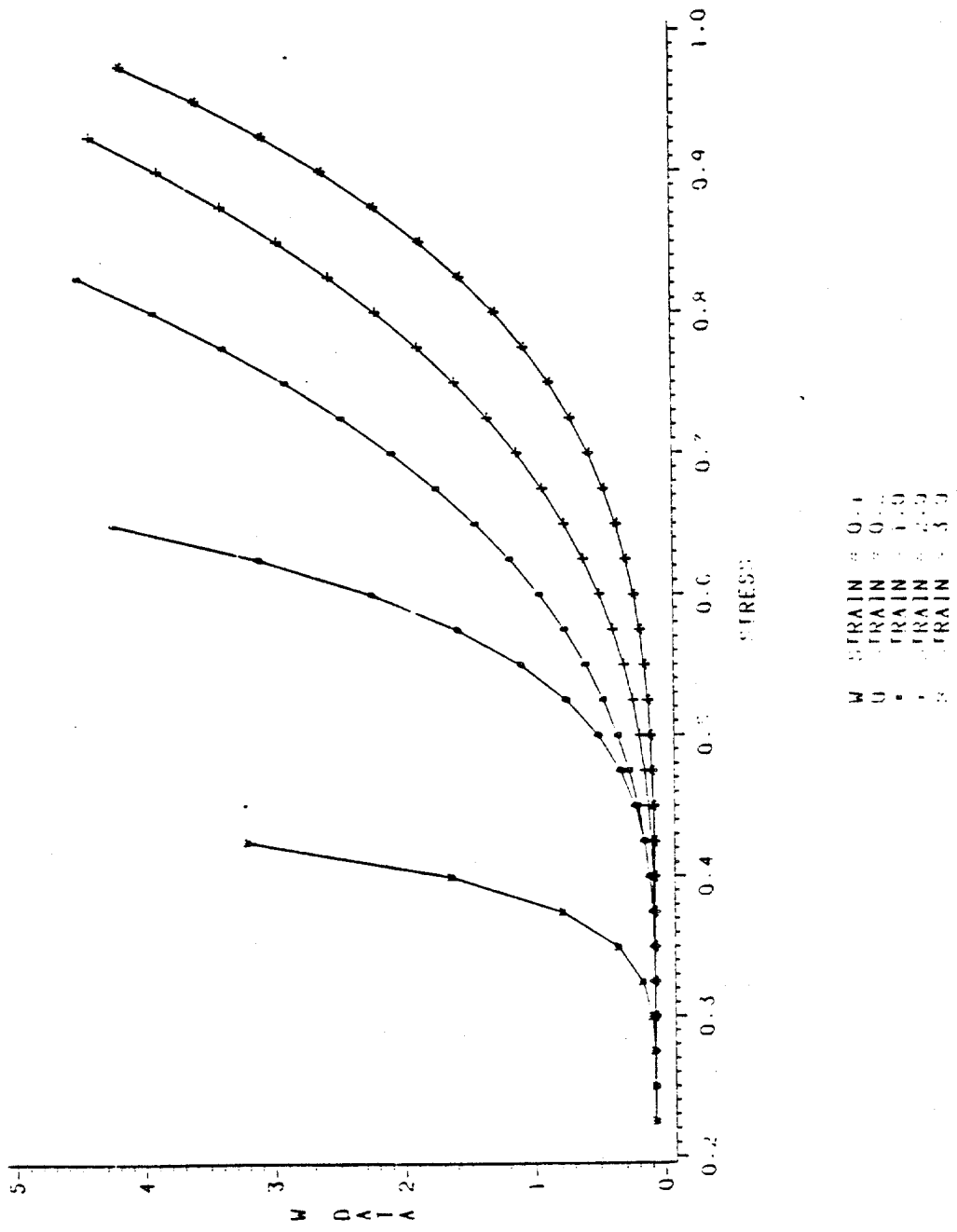


Fig. 16 - Planes of constant strain for the W data function.

# W DATA FUNCTION CONSTANT STRESS PLANES

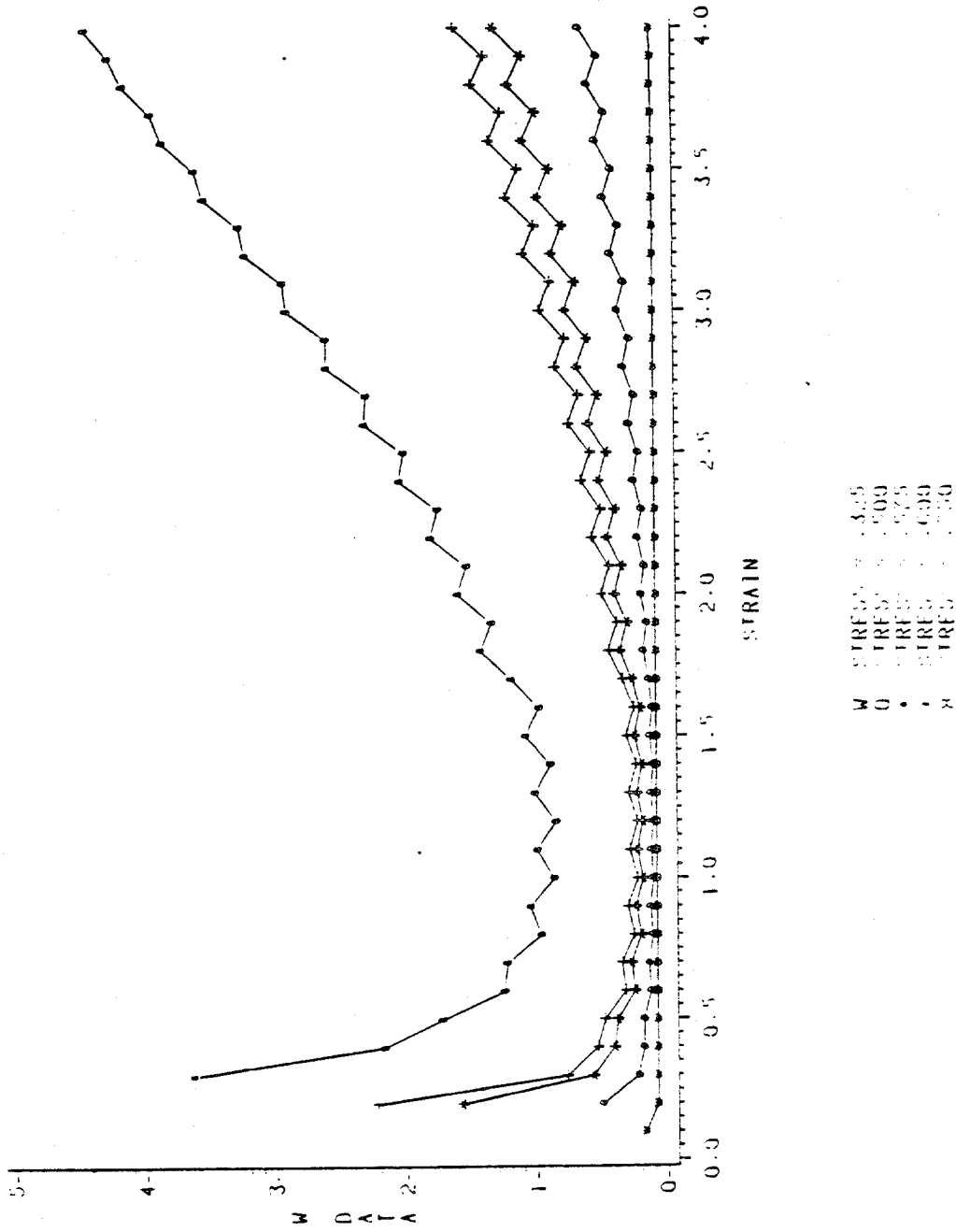


Fig. 17 - Planes of constant stress for the W data function.

# Y DATA FUNCTION

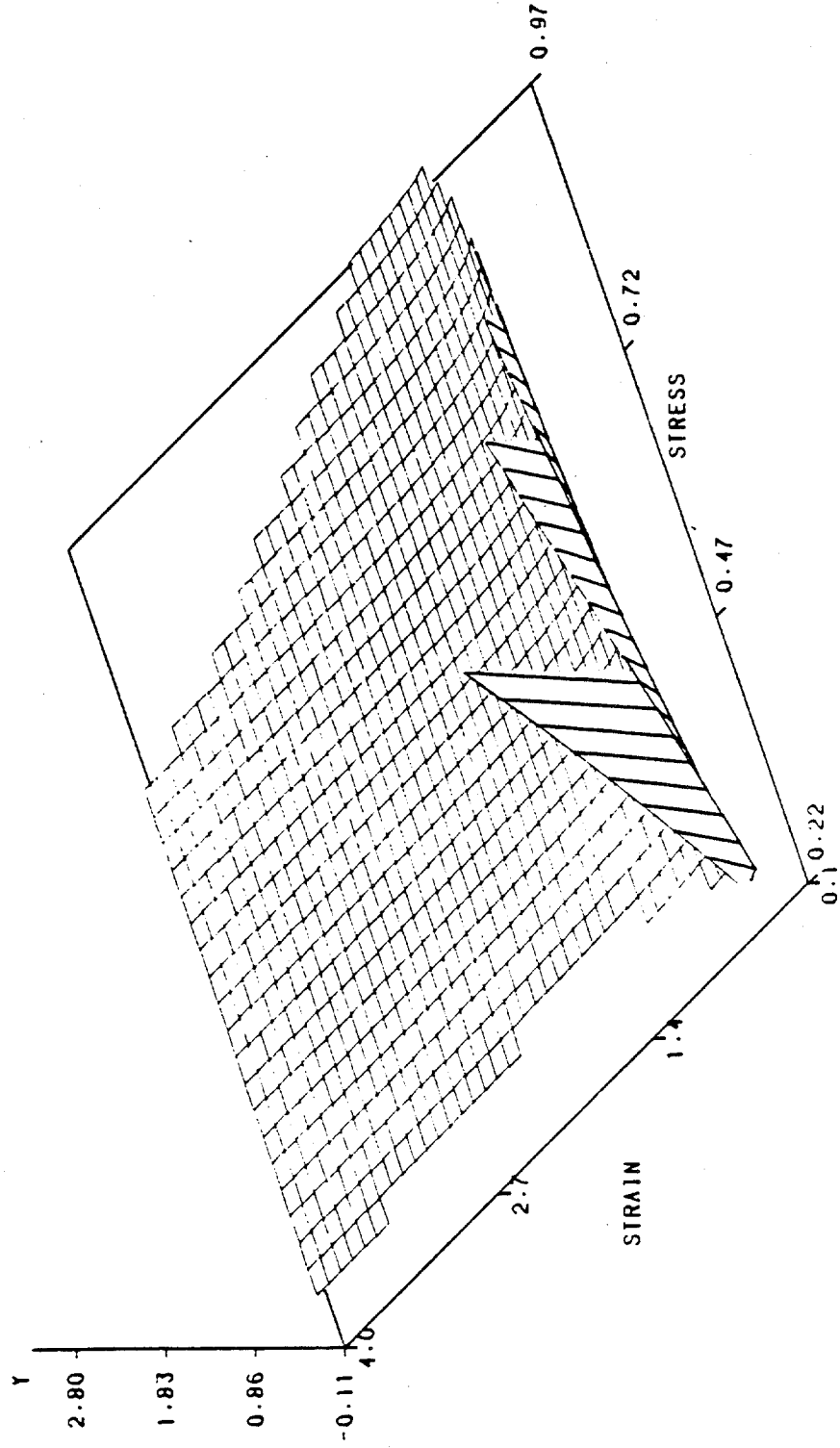


Fig. 18 - Three-dimensional representation of the Y data function.

# Y DATA FUNCTION CONSTANT STRAIN PLANES

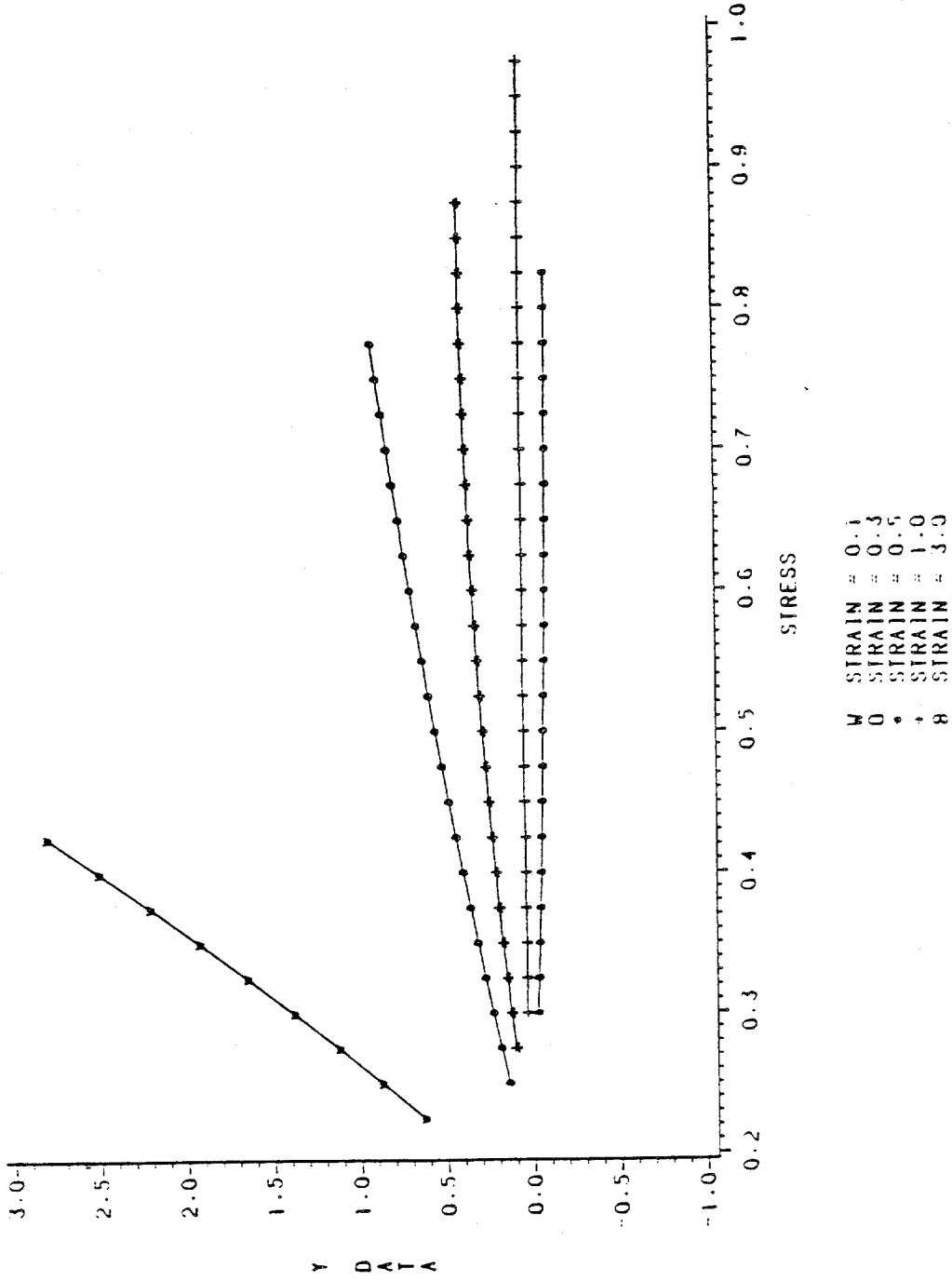


Fig. 19 - Planes of constant strain for the Y data function.

# Y DATA FUNCTION CONSTANT STRESS PLANES

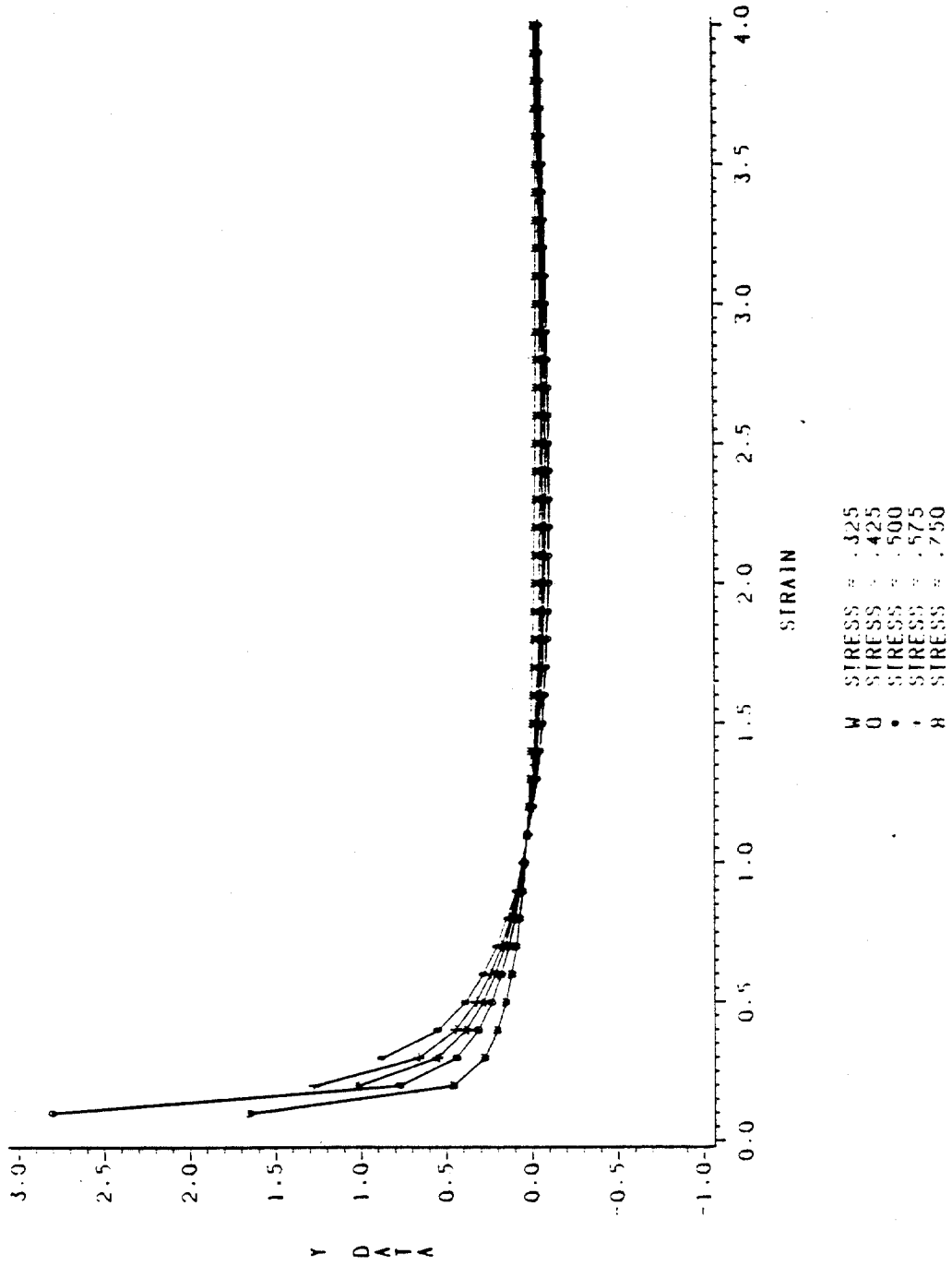


Fig. 20 - Planes of constant stress for the Y data function.

RESPONSE FUNCTIONS

In the previous section, the three data functions  $F(s,e)$ ,  $W(s,e)$  and  $Y(s,e)$  are determined from families of constant load and constant strain rate tests. The task now is to determine the material response functions  $\omega(s,e)$ ,  $\phi(s,e)$  and  $\psi(s,e)$  from the data functions. From the two types of tests considered, the response functions are related to the data functions by equations (5) and (8). From these equations we see that the two test types only provide two independent relations from which to determine the three response functions.

Morland<sup>2</sup> investigates other uniaxial test types (i.e., constant displacement and constant load rate tests) in an effort to find a third independent relation to uncouple the response functions. He finds that regardless of the test type chosen, only two relations can be independent, since the uniaxial stress response defined by equation (2) can be expressed in a form involving only two combinations of the coefficients. The form depends on the two types of tests chosen to measure the data functions. If the constant strain rate and constant load tests are chosen, then equation (2) can be reduced to the form,

$$\dot{\sigma} = \hat{Y} (\dot{\epsilon} - F), \quad (14)$$

where  $\hat{Y}$  is a combination of  $F$ ,  $W$ , and  $Y$ .

The simple form in (14) is obtained by dividing the uniaxial stress relation in (2) by a function of  $(s,e)$ . This division reduces the number of coefficients from three to two. In the general tensor relation this division is not possible and the function remains as a distinct quantity which governs the separation of  $\hat{\phi}$  and  $\hat{\omega}$  into the quantities  $\phi_1$ ,  $\phi_2$ ,  $\omega_1$ ,  $\omega_2$ . The separation of  $\hat{\phi}$  and  $\hat{\omega}$  along with  $\psi$  provides the five independent coefficients necessary to describe the deformation of an incompressible material. These coefficients must be determined from a program of multiaxial tests. If these coefficients were known, then the composition of  $\hat{\phi}$  and  $\hat{\omega}$  could be determined which would, in turn, yield the uniaxial stress model defined in (2).

REDUCED UNIAXIAL MODELS

Despite the necessity of having multiaxial data to describe the uniaxial stress model described by Equation (2), Morland<sup>2</sup> suggests three reduced models which can be determined by uniaxial data alone. These reduced models depend on certain assumptions about the functional dependence of the response functions. The assumptions provide a third equation necessary to uncouple the three response functions appearing in Equations (5) and (8).

The first reduced model considers the removal of terms in (2) by setting the  $\hat{\phi}$ ,  $\hat{\psi}$  and  $\hat{\omega}$  equal to zero in turn. Setting  $\hat{\phi} = 0$  leads to a contradiction involving the elastic jump and  $\hat{\psi} = 0$  leads to a physically unacceptable response for the constant displacement test. For  $\hat{\omega} = 0$ , there is no explicit dependence on the strain tensor, but dependence on strain is maintained through the arguments of  $\hat{\phi}$  and  $\hat{\psi}$ . The absence of  $\hat{\omega}$  in (2) implies that upon complete unloading from any stress-strain state there is an elastic strain decrease but no subsequent creep relaxation. Whether or not this is an acceptable approximation needs to be determined from experimental data. If  $\hat{\omega} = 0$  is an acceptable approximation, then  $\hat{\phi}$  and  $\hat{\psi}$  can be determined from Equations (5) and (8) which yield,

$$\hat{\psi} = \frac{s}{\hat{Y}} , \quad \hat{\phi} = \frac{2s(1-e)}{3\hat{Y}} \{ (1-e)\hat{Y} - 2s \} . \quad (15)$$

This reduced model, however, is not acceptable. The functions  $\hat{\psi}$  and  $\hat{\phi}$  in (15) become unbounded since  $\hat{Y} \rightarrow 0$  at points which correspond to the peak values of any stress-strain curves.

Morland<sup>2</sup> suggests an alternate approach for obtaining reduced models by restricting the dependence of the response coefficients  $\hat{\psi}$ ,  $\hat{\omega}$  and  $\hat{\phi}$  on  $s$  and  $e$ . These restrictions can be obtained by measuring the creep recovery upon complete unloading from some current state  $(s_1, e_1)$  at the time  $t_1/t_s$ . In this case, we have,

$$t/t_s > t_1/t_s : s = 0, \quad \dot{e} = F(0, e) = -f(e) < 0, \quad e \left( \frac{t_1}{t_s} \right) = e_1^+ , \quad (16)$$

where  $e_1 - e_1^+$ , is the elastic strain decrease. Here  $f(e)$  measures the strain rate response of the material upon unloading and is necessarily independent of the stress  $s_1$ . In the absence of unloading data, we would expect the unloading response to be similar to the response shown in Figure 21(a). As  $t \rightarrow \infty$ ,

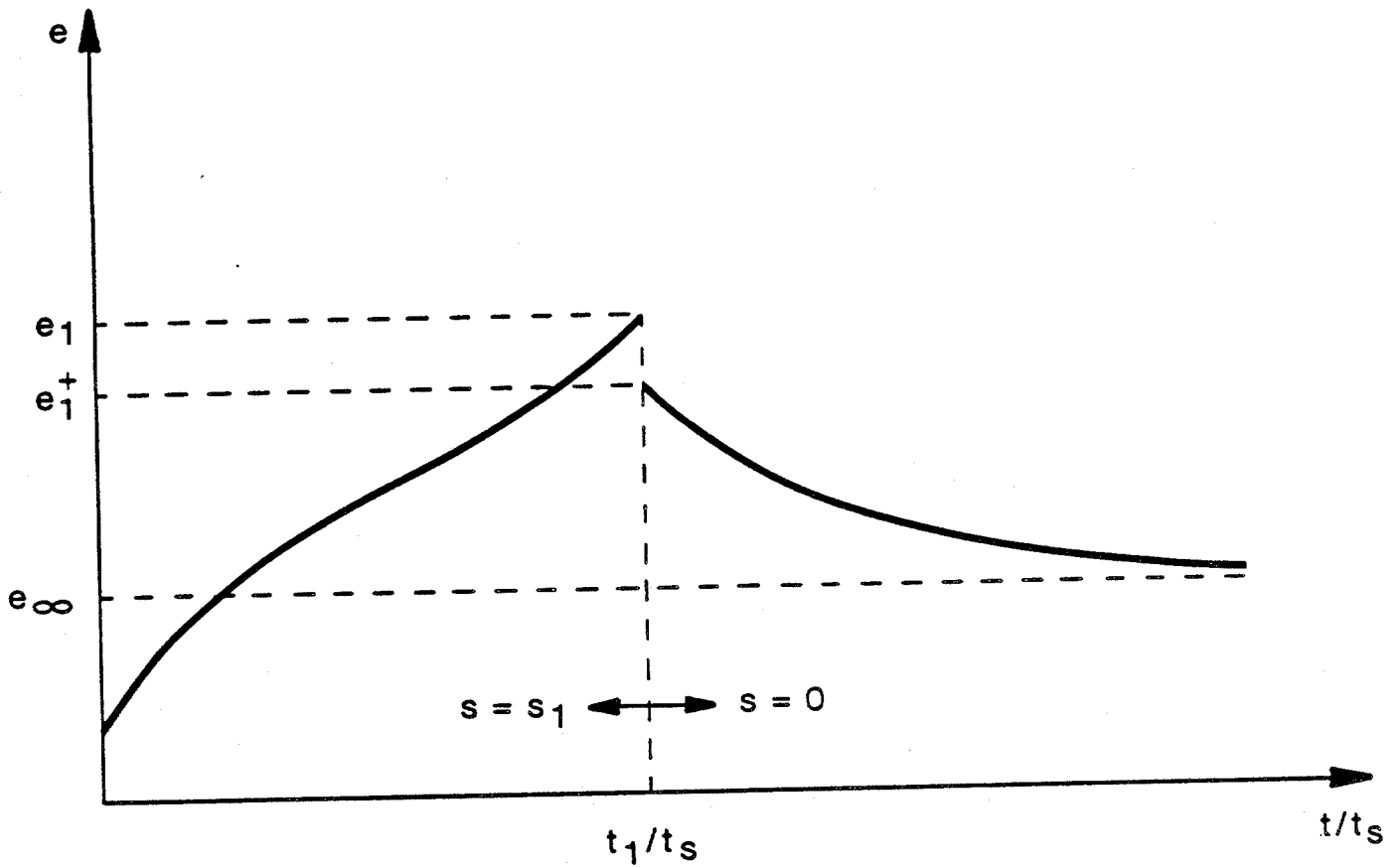


Fig. 21a - Expected creep response of ice upon unloading.

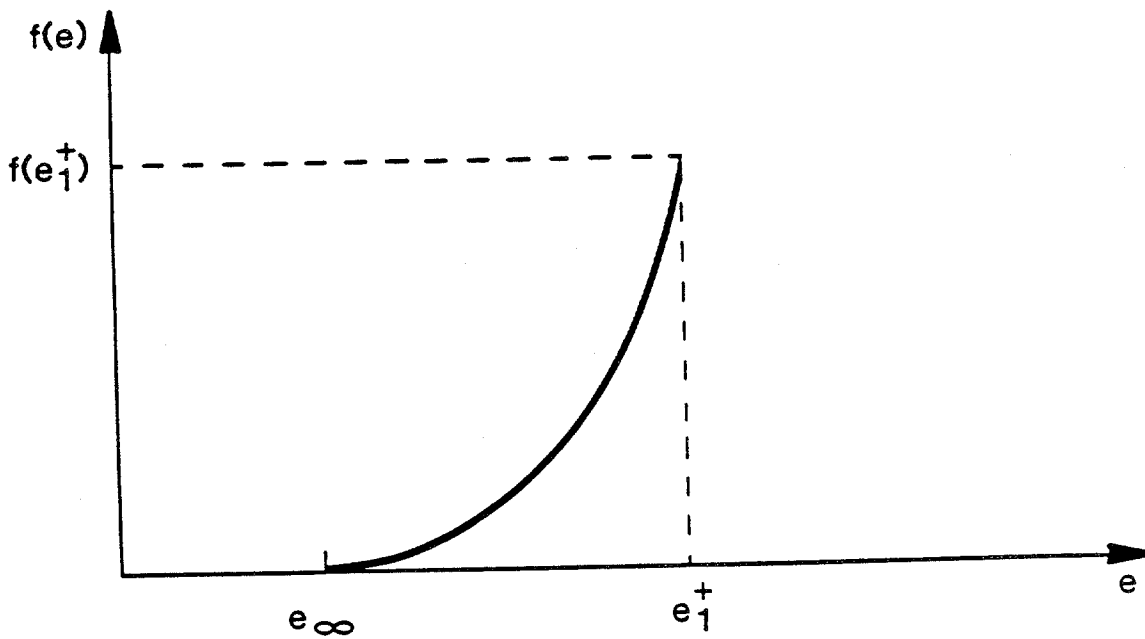


Fig. 21b - Expected shape of  $f(e)$ .

$f(e) \rightarrow 0$  and the material recovers to some permanent strain  $e_{\infty}$ . The expected shape of  $f(e)$  is shown in Figure 21(b) which can be approximated by a power law of the form,

$$f(e) = f_0 \left( \frac{e - e_{\infty}}{e_1^+ - e_{\infty}} \right)^n, \quad e_{\infty} \leq e \leq e_1^+, \quad n \geq 1 \quad (17)$$

The values of  $f_0$ ,  $n$ ,  $e$ ,  $e_1^+$ , and  $e_{\infty}$  would depend on the history of loading and the elastic jump from  $e_1$  to  $e_1^+$ . Since  $f(e)$  depends implicitly on loading history, many unloading tests would have to be conducted for different values of  $(s_1, e_1)$  before  $f(e)$  could be determined.

In his investigation of the strain rate response  $f(e)$ , Morland<sup>2</sup> concludes that complete recovery is necessary and, hence,  $e_{\infty}$  in (17) must equal zero. However, in general one would expect  $e_{\infty} \neq 0$  since creep tests under large applied loads induce deformation mechanisms such as microcracks which would be irreversible upon unloading. Whether or not  $e_{\infty} = 0$  is an acceptable approximation needs to be determined experimentally.

From equations (5) and (8), we have

$$f(e) = \frac{\hat{\omega}(0, e)e}{\frac{3}{2}(1 - e)\hat{\phi}(0, e)} \quad (18)$$

Thus, the relaxation function  $f(e)$  determines the ratio  $\hat{\omega}(0, e)/\hat{\phi}(0, e)$  evaluated at zero stress. If we assume that  $\hat{\omega}/\hat{\phi}$  is in general independent of stress and, hence, given by  $f(e)$ , then a third independent relation for the response functions is obtained. From equations (5), (8), and (18) we find,

$$\hat{\omega}e = \frac{3}{2} \hat{\phi}(1 - e)f, \quad \hat{\psi} = \frac{\frac{3}{2} \hat{\phi}}{(1 - e)^2 \hat{Y} - 2(1 - e)s} \quad (19)$$

$$\frac{3}{2} \hat{\phi} = \frac{(1 - e)^2 s \{(1 - e)\hat{Y} - 2s\}}{2sF + (F + f)\{(1 - e)\hat{Y} - 2s\}}$$

In order to evaluate the response functions in (19), values for the parameters defining  $f(e)$  in (17) must be assumed due to the lack of experimental data. We assume that upon unloading, there is a complete recovery, i.e., we assume  $e_{\infty} = 0$ . Furthermore, we assume that the initial value of  $f(e)$

is obtained at the strain state  $e_1^+ = 4.0$ . This guarantees that  $f(e)$  is defined everywhere in our strain domain,  $0 < e \leq 4.0$ . We arbitrarily choose  $f_0 = 1.0$  and  $n = 2$ . With these assumptions, three-dimensional plots for the three response functions can be obtained. Figures 22-24 illustrate the response functions  $\hat{\phi}$ ,  $\hat{\omega}$ , and  $\hat{\psi}$ , respectively. These figures show that the assumption  $\hat{\omega}/\hat{\phi} = f(e)$  leads to singularities in the response functions.

Further simplifications for the response functions in (19) can be made by recognizing that elastic strains associated with a stress jump,  $s$ , are infinitesimal, i.e.,  $s/\hat{Y} \ll 1$ . Neglecting  $s/\hat{Y}$  compared to unity yields

$$\hat{Y} = \frac{3\hat{\phi}}{2(1-e)^2\hat{\psi}} \quad (20)$$

which implies  $\hat{\phi} \gg \hat{\sigma}\hat{\psi}$ . This approximation leads to the following simplification for  $F$  and the response function:

$$F = \frac{(1-e)^3 s - \hat{\omega}e}{\frac{3}{2}\hat{\phi}(1-e)} \quad (21)$$

$$\frac{3}{2}\hat{\phi} = \frac{(1-e)^2 s}{F+f} \quad , \quad \hat{\psi} = \frac{s}{(F+f)\hat{Y}} \quad , \quad \hat{\omega}e = \frac{(1-e)^3 s f}{F+f} \quad .$$

This simplification is also unacceptable since  $\hat{\psi}$  becomes unbounded as  $\hat{Y} \rightarrow 0$  near points which correspond to points of peak stress in a constant strain rate test.

Morland<sup>2</sup> proposes a third reduced model which follows a development parallel to the second model. The third reduced model is obtained by dividing Equation (2) by  $\hat{\psi}$ . This normalized reduced model is,

$$(1-e)\dot{s} - 2(1-e)^2 s \dot{e} + (1-e)^3 \hat{\psi}^* s = \frac{3}{2} \hat{\phi}^* (1-e) \dot{e} + \hat{\omega}^* e \quad , \quad (22)$$

where

$$\hat{\psi}^* = \frac{1}{\hat{\psi}} \quad , \quad \hat{\phi}^* = \frac{\hat{\phi}}{\hat{\psi}} \quad , \quad \hat{\omega}^* = \frac{\hat{\omega}}{\hat{\psi}} \quad .$$

This third model can also be constructed with one-dimensional data alone provided unloading data are available, i.e.,  $f(e)$  must be measured.

# PHI RESPONSE FUNCTION

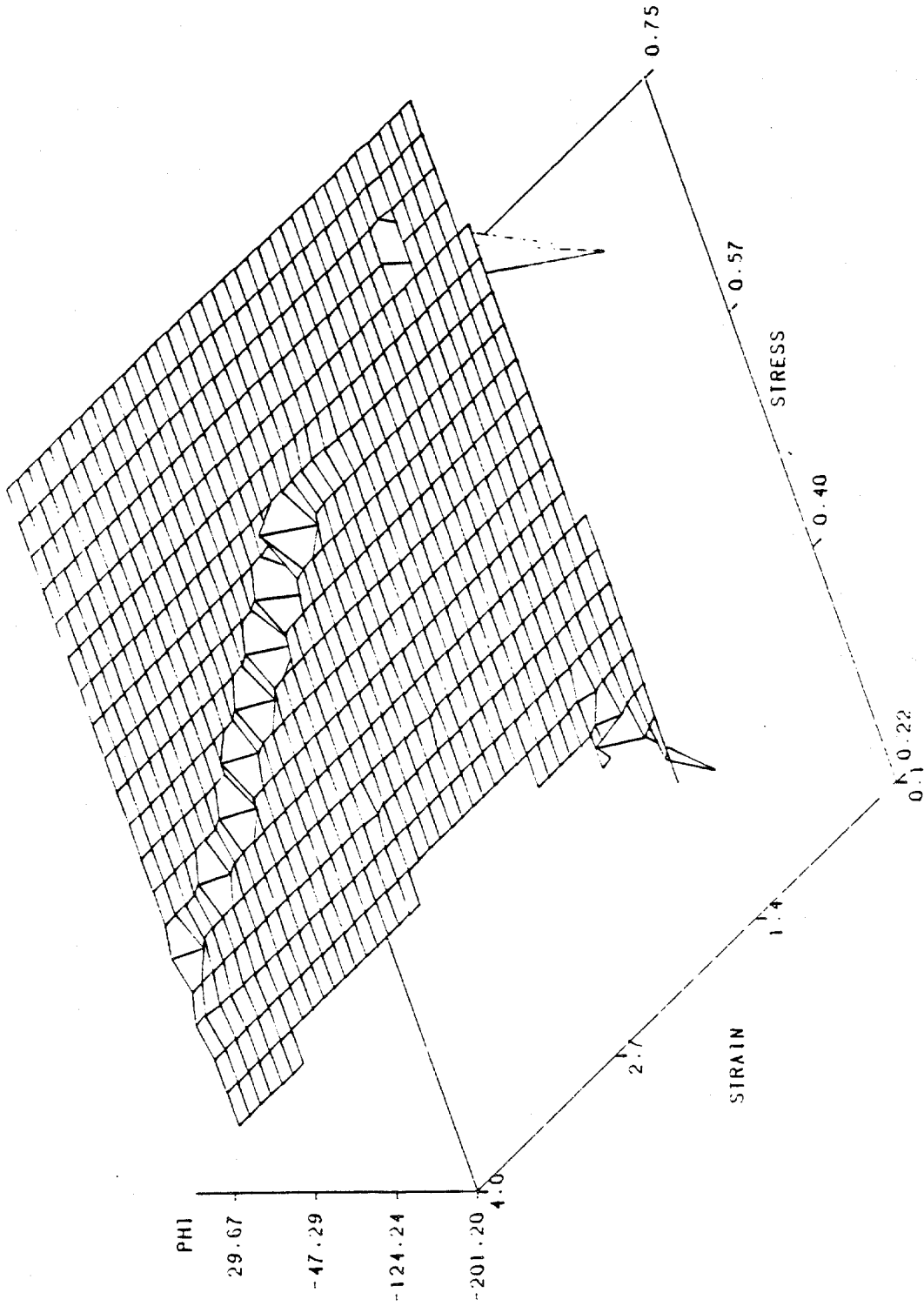


Fig. 22 - Three-dimensional representation of the response function  $\hat{\phi}(s, e)$  based on the reduced model,  $\omega/\phi = f(e)$ .

# OMEGA RESPONSE FUNCTION

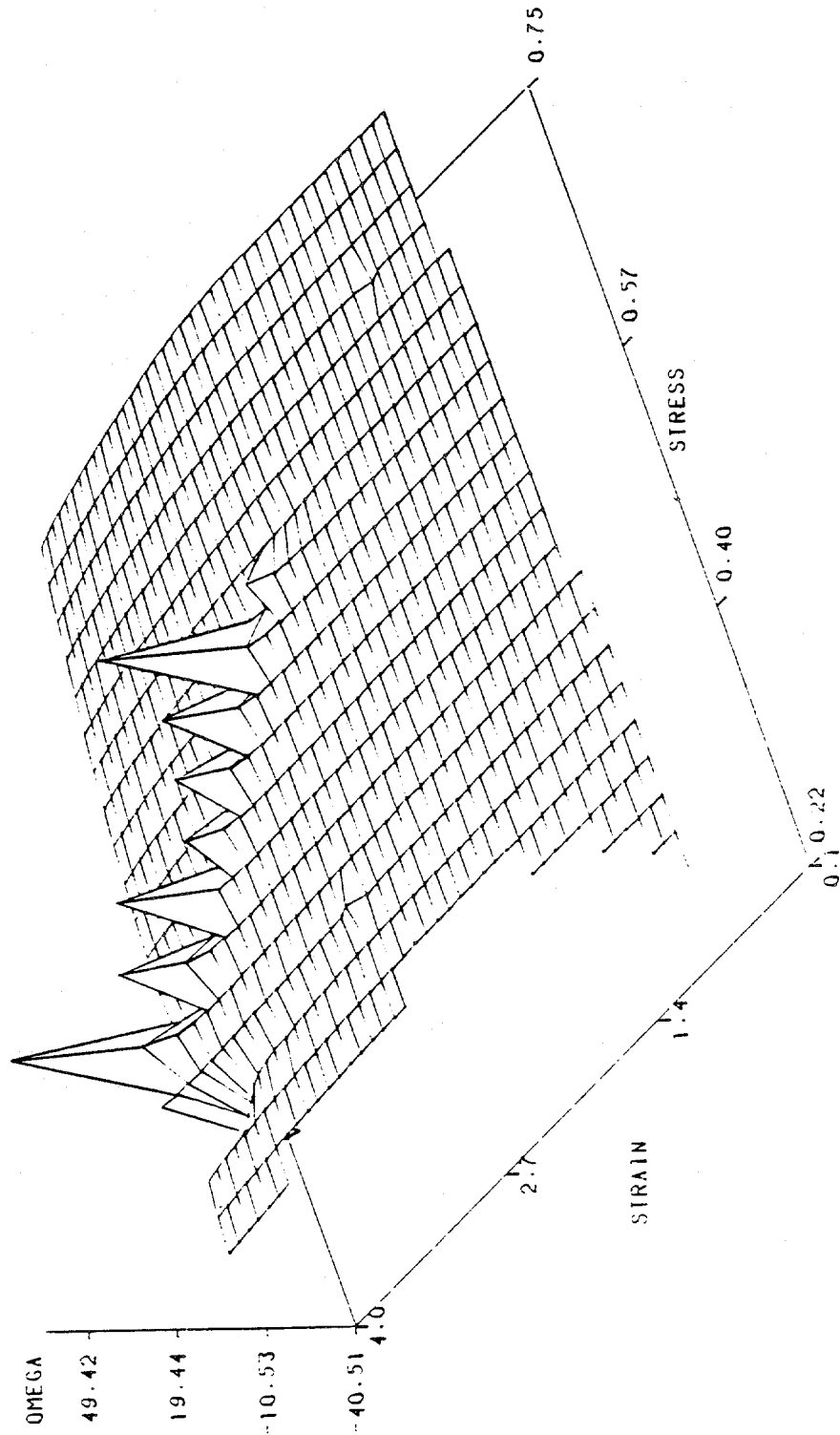


Fig. 23 - Three-dimensional representation of the response function  $\hat{\omega}(s, e)$  based on the reduced model,  $\omega/\phi = f(e)$ .

# PSI RESPONSE FUNCTION

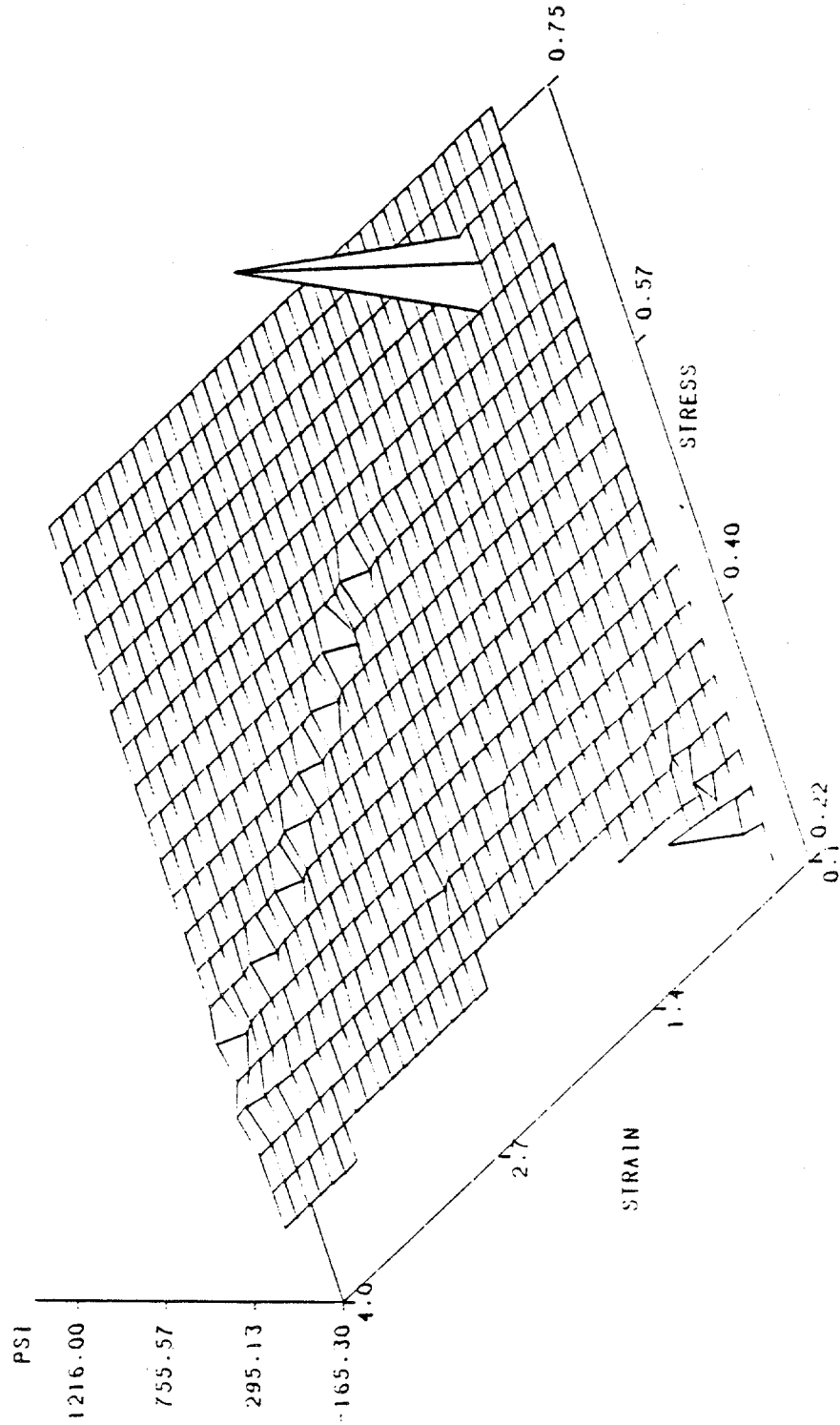


Fig. 24 - Three-dimensional representation of the response function  $\hat{\psi}(s,e)$  based on the reduced model,  $\omega/\phi = f(e)$ .

The simplifications resulting from neglecting  $s/\hat{Y}$  compared to unity and which correspond to Equation (21) are,

$$F = \frac{(1 - e)^3 s \hat{\psi}^* - \hat{\omega}^* e}{\frac{3}{2} \hat{\phi}^* (1 - e)}$$

$$\frac{3}{2} \hat{\phi}^* = (1 - e)^2 \hat{Y}, \quad \hat{\psi}^* = \frac{(F + f) \hat{Y}}{s}, \quad \hat{\omega}^* e = (1 - e)^3 \hat{Y} f.$$

Note that this model depends on  $(F + f)$  approaching zero as fast or faster than  $s$  for  $\hat{\psi}^*$  to be bounded. However, data are not available to investigate this limit.

Further simplifications of the second and third models can be made by assuming  $\hat{\phi}$  and  $\hat{\omega}$  (or  $\hat{\phi}^*$  and  $\hat{\omega}^*$ ) to be separable functions of stress and strain. Pursuit of these models would be a meaningless exercise without experimental measurement of  $f(e)$ . The reader is referred to Morland for development of these models.

The three reduced one-dimensional models introduced by Morland<sup>2</sup> are either unacceptable due to singularities or incomplete due to lack of data. It may be possible to devise other reduced models, but further investigations would be needed. It is doubtful that other such reduced models will be suitable, since the original model is the simplest tensorial relation necessary to describe the observed response of ice. Reduction of this "simplest" model would probably eliminate certain key features of the material's response. Thus, the satisfactory development of a one-dimensional model will probably require multiaxial data.

#### STRESS-STRAIN DOMAIN FOR RESPONSE FUNCTIONS

Regardless of whether the response functions are determined from a suitable reduced model or from multiaxial data, their construction would permit the solution of initial boundary value problems involving uniaxial states of stress. Of course, solutions to these problems can only be obtained in stress-strain domains where the response functions are defined. The domain of definition is simply the intersection of the stress-strain domain for the data functions illustrated in Figures 7 and 13. The intersection of these domains is shown in Figure 25.

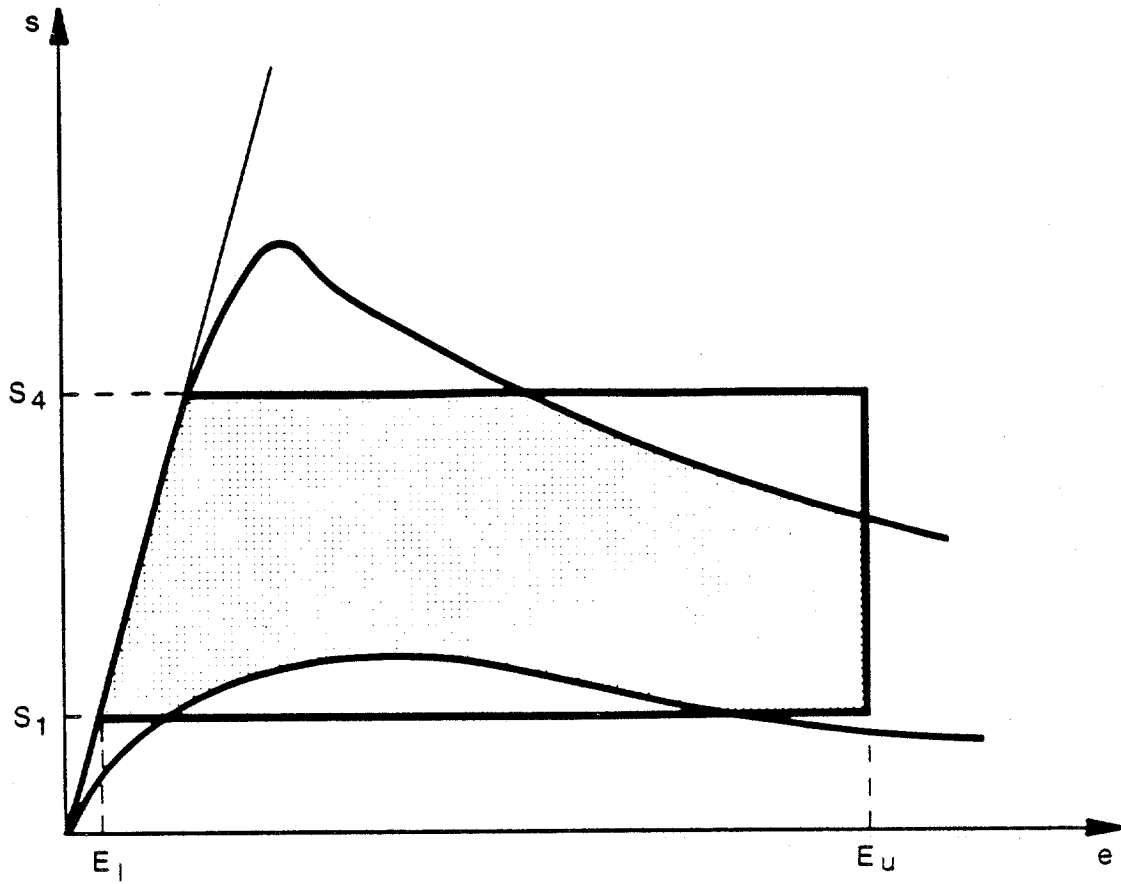


Fig. 25 - Stress-strain domains for the response functions.

From Figure 25, the stress-strain domain for the response function is rather restricted and should be extended in order to solve problems of a general nature. In particular, the extension of the domain to include the origin is necessary to solve problems where the initial state of the ice is undeformed and stress free. For these problems, the initial values of the data functions must be evaluated.

From equation (5), we find  $F(s,e) \rightarrow 0$  as  $(s,e) \rightarrow (0,0)$ , and since we have restricted the initial response of the constant strain rate tests to be elastic, we have  $Y(s,e) \rightarrow \bar{Y}$  as  $(s,e) \rightarrow (0,0)$ . Thus, both  $F(s,e)$  and  $Y(s,e)$  are defined and unique at  $(s,e) = (0,0)$ .

However, since  $W(s,e)$  represents the strain rate of a constant strain rate test, its value at the origin is nonunique. This is not surprising, since the strain rate of an idealized constant strain rate test is a step function at the origin. A unique  $W$  at the origin would require dependence on the stress rate. This would, in turn, require general rate dependence of the other data functions. To maintain rate independence of the data functions, a unique value of  $W$  can be artificially imposed at the origin. A candidate for this value is obtained by redefining  $W(s,e)$  to be,

$$W(s,e) = (W_4 - W_j)e^{Y(s,e) - \bar{Y}} + W_j. \quad (24)$$

Here  $W_j$ ,  $j = 1,4$  ( $W_1 < W_2 < W_3 < W_4$ ) are the strain rates associated with each stress-strain curve in our family of constant strain rate tests.

Equation (20) couples the strain rate  $W(s,e)$  with the stress-strain gradient  $Y(s,e)$ . Since  $Y(0,0) = \bar{Y}$ , the value of  $W(0,0)$  is the highest strain rate of our family of constant strain rate tests. Since high strain rates are associated with an elastic response, this equation is consistent with our assumption that the initial response is elastic. As the current  $(s,e)$  point moves away from the origin, the first term of equation (20) decays exponentially to zero. This decay should be sufficiently fast to guarantee that the proper definition of  $W(s,e)$  prevails at points away from the origin.

With the definition of  $W$  in equation (20), all response functions are defined at the origin. We now need to investigate the data functions near the stress and strain axes. Consider first the strain axis. The data function  $F(0,e)$  cannot be determined by the constant load test,  $s = 0$ , since if no load is applied, there will be no measured response, i.e.,  $F(0,e) = 0$ .

This implies that upon complete unloading there would be an elastic strain decrease but no subsequent creep recovery. Instead, the function  $F(o,e) = -f(e) < 0$  must be measured by complete unloading from some state  $(s_1, e_1)$ . If the measured response  $f(e)$  depends appreciably on the stress before unloading then the response functions depending only on stress and strain are unsatisfactory.

To extend the data functions  $W$  and  $Y$  toward the strain axis, we need to obtain stress-strain curves from tests conducted at increasingly small strain rates. As the strain rate decreases, we would expect the stress-strain curve to collapse toward the strain axis. Hence, we would expect  $Y(s,e) \rightarrow 0$  and  $W(s,e) \rightarrow 0$  as  $s \rightarrow 0$ . However, since we have specified nonzero values of  $Y$  and  $W$  at the origin, the data functions at best can only be defined along the strain axis for some small value,  $s = 0^+$ . This is satisfactory as long as the current stress-strain point lies in the quadrant  $s > 0, e > 0$ . If the current stress-strain point moves across the strain axis, then the data functions  $W$  and  $Y$  must be redefined at the origin. This would require the response functions to be rate dependent.

Finally, consider the stress axis  $(s,0)$ . When defining the stress-strain domains of the constant load and constant strain rate tests, we saw that all permissible responses were restricted to domains to the right of the line  $s = \bar{Y}e$ . Responses corresponding to points to the left of this line can be obtained from nonmonotonic load paths. Consider a tension compression load path:

$$\begin{array}{ll} 0 \leq t \leq t_1 & s = -T < 0 \text{ (tension)} \\ t > t_1 & s = P > 0 \text{ (compression)}. \end{array}$$

During the tension stage there will be an elastic tension strain jump followed by tensile creep resulting in a total tensile strain  $e = e_1 < 0$  at  $t = t_1$ . At  $t = t_1$  the stress jump  $P + T$  will cause an elastic compressive strain jump followed by compressive creep. The relative magnitudes of the compressive and tensile loads can be adjusted so that the compressive creep responses correspond to points to the left of  $s = \bar{Y}e$ .

### SUMMARY AND RECOMMENDATIONS

A nonlinear viscoelastic law of the differential type has been developed by Spring and Morland<sup>3</sup> to describe the mechanical behavior of ice. This constitutive law represents the simplest differential equation necessary to describe the observed behavior of ice under constant load and constant strain rate conditions. As a first step in applying this law to the solution of ice structure interaction problems, Morland<sup>2</sup> investigates the uniaxial stress reduction of the general tensor relation in (1). The uniaxial model requires the measurement of three data functions from a family of uniaxial constant load and constant strain rate tests. These data functions are related to three response functions which appear directly in uniaxial stress reduction of the governing differential equation. Morland assumes that both the data and response functions are functions of stress and strain.

Although there are three measured data functions and three undetermined response functions, Morland<sup>2</sup> shows that any uniaxial testing program will only provide two independent equations relating the data and response functions. Consequently, multiaxial data are required to uncouple the response functions. Morland suggests some assumptions regarding the functional dependence of the response functions which permit the construction of three reduced uniaxial models from uniaxial data alone.

The work presented here describes the procedures followed to construct the reduced uniaxial models from experimental data. The data chosen for this study are from the tests conducted by Mellor and Cole<sup>4</sup> on fine grained polycrystalline ice. Four constant load and four constant strain rate tests were chosen from the data set to construct the three data functions. Construction of the three reduced uniaxial models from the data functions was unsuccessful. It appears that a suitable uniaxial model will require multiaxial data.

The domain over which the data functions are defined is restricted to a small domain in the compression quadrant,  $s \geq 0$ ,  $e \geq 0$ , of the stress-strain plane. The ability to solve problems of general interest requires this domain to be extended to at least the entire compression quadrant. Extension of the domain toward the origin reveals nonuniqueness of a data function there. Uniqueness of this function at the origin would require general dependence of the response function on stress, strain and their rates. Rather than reformulate the response functions with rate dependence, a unique value

at the origin is imposed on the data function. Further theoretical work should be done to ensure that this approach does not lead to contradictions for any arbitrary approach toward the origin. To extend the domain of definition toward the stress and strain axes, additional tests need to be conducted. These are specialized tests involving unloading and tension-compression load paths. Extension of the domain outside of the compression quadrant would require further theoretical and experimental work.

Once all theoretical questions are resolved and the additional laboratory data are obtained, much effort is still required to develop the numerical procedures necessary to use the nonlinear one-dimensional material model. Even if these problems are solved, important features of ice's behavior, such as pressure dependence, are omitted. The inclusion of pressure dependence in the model, for example, would require the generalization of the response functions to include dependence on the stress and strain invariants. An extensive multiaxial test program would then be required to evaluate the generalized response functions.

It is clear that in order to develop the constitutive model discussed here into a useful tool for calculating ice loads, extensive additional theoretical, experimental, and numerical work needs to be done. The implementation of the model would require the allocation of large amounts of resources and manpower which would not yield results for quite some time. Even if such allocations were made, implementation of the model would probably be limited to laboratory ice given the variability of properties in natural ice. For these reasons, further work on this model does not seem promising.

#### REFERENCES

1. Cox, G. F. N., Richter-Menge, J. A., Weeks, W. F., Mellor, M., and Bosworth, H. W. (1983), The Mechanical Properties of Multi-Year Sea Ice, Phase I: Test Results, Report 84-9, Cold Regions Res. Eng. Lab., Hanover, N.H.
2. Morland, L. W. (1981), Mechanical Properties of Sea Ice Theoretical Phase, September 1980-November 1981, Consultants report submitted to Shell Development Company, confidential until January 1, 1985.
3. Spring, U. and Morland, L. W. (1982), Viscoelastic Solid Relations for the Deformation of Ice, Cold Regions Sci. Technol., v. 5, No. 3.
4. Mellor, M. and Cole, D. M. (1982), Deformation and Failure of Ice Under Constant Stress or Constant Strain Rate, Cold Regions Sci. Technol., v. 5, No. 3.

